

**Luminescent films for chemo- and biosensing**

Journal:	<i>Chemical Society Reviews</i>
Manuscript ID:	CS-REV-03-2015-000246.R1
Article Type:	Review Article
Date Submitted by the Author:	15-Jun-2015
Complete List of Authors:	Guan, Weijiang; State Key Laboratory of Chemical Resource Engineering, Beijing University of Chemical Technology Zhou, Wenjuan; State Key Laboratory of Chemical Resource Engineering, Beijing University of Chemical Technology Lu, Jun; Beijing University of Chemical Technology, State Key Laboratory of Chemical Resource Engineering Lu, Chao; School of Science,



Chem Soc Rev

REVIEW ARTICLE

Luminescent films for chemo- and biosensing

Received 00th January 20xx,
Accepted 00th January 20xx

DOI: 10.1039/x0xx00000x

www.rsc.org/

Weijiang Guan, Wenjuan Zhou, Jun Lu and Chao Lu*

Luminescent films have received great interest for chemo-/bio-sensing applications due to their distinct advantages over the solution-based probes, such as good stability and portability, tunable shape and size, non-invasion, real-time detection, extensive suitability in gas/vapor sensing, and recycling. On the other hand, they can achieve selective and sensitive detection of chemical/biological species using special luminophores with recognition moiety or the assembly of common luminophores and functional materials. Nowadays, the extensively used assembly techniques include drop-casting/spin-coating, Langmuir–Blodgett (LB), self-assembled monolayers (SAMs), layer-by-layer (LBL), and electrospinning. Therefore, this review summarized the recent advances in luminescent films with these assembly techniques and their applications in chemo-/bio-sensing. We mainly focused on the discussions of the relationship between the sensing properties of the films and their architecture. Furthermore, we discussed some critical challenges existing in this field and possible solutions that have been or are being developed to overcome these challenges.

1. Introduction

As a fascinating visual phenomenon, analyte-induced luminescence switching has become one of the most intuitive manners to quantitate chemical/biological species.^{1–3} Nowadays, huge amounts of luminescent chemo-/bio-probes in solution have been successfully developed. However, most of them are made of organic small molecule luminophores^{4–6} and fluorescent conjugated polymers^{7–9} with an inherent hydrophobicity. However, it is difficult to make the hydrophobic luminophores hydrophilic with unchangeable functions.^{10–12} Actually, the majority of the analytes especially metal ions and biological samples,^{2,3} usually exist in aqueous systems. On the other hand, the development of inorganic luminophores with water-soluble ligands, such as quantum dots (QDs)^{13–15} and luminescent metal nanoclusters (NCs)^{16,17}, seems to be an alternative method but encounters new problems (*e.g.*, limited variety). In addition, the water-soluble probes in solution also exhibit some inborn shortcomings, impeding their extensive applications: (1) the solution-based luminescence platform is inconvenient to store and transport,^{18,19} (2) the water-soluble probes cannot be recyclingly used because they are not easy to be separated from the analytes in solution,^{20–22} (3) the random disposal of these one-off probes leads to the reagent consumption and environmental pollution,^{23,24} (4) for the biological samples (*e.g.*, cell and tissue), the water-soluble

probes might induce unexpected chemicals released from biological samples;²⁵ (5) the water-soluble probes are difficult to be used for vapor/gas detection.^{26–28}

In the past several decades, it is preferable to develop luminescent films consisting of various kinds of luminophores and functional materials to overcome these drawbacks of luminescence probes in solution for chemo-/bio-sensing. Luminescent films can be transformed easily into the device format with several unique advantages: (1) luminescent films with any shape and size (dependent on the substrate pattern) can be easily fabricated for various needs and occasions;^{29–31} (2) they are easy to store and transport as a result of the good chemical stability of luminophores in the solid state;^{32,33} (3) there does not exist the invasive interferences since the detection is usually performed in the luminescent films with no external addition;^{25,34} (4) luminescent films enable real-time detection of the analyte;^{35–37} (5) luminescent films can be regenerated by washing them with suitable solvents.^{38–40} A successful luminescent film in chemo-/bio-sensing should exhibit high selectivity and sensitivity. There are two major strategies of selective sensing in the design of luminescent films. The direct strategy is to synthesize the luminophores with recognition moiety, as similar to the solution-based probes.^{41–43} Alternatively, the luminophores can be assembled with recognition units through a variety of physical interactions with little or no synthetic efforts.^{44–46} Thanks to the strategy of assembly, the fabrication of luminescent films becomes more flexible and diverse. For the sensitivity, aggregation-caused quenching (ACQ) effect is a main obstacle for detection sensitivity during the formation of luminescent films, in which the luminophores inherently tend to aggregate through intermolecular π - π interactions.^{47–49} Aggregation-induced

State Key Laboratory of Chemical Resource Engineering, Beijing University of

Chemical Technology, Beijing 100029, China. E-mail: luchao@mail.buct.edu.cn;

Fax: +86 010 64411957; Tel: +86 010 64411957

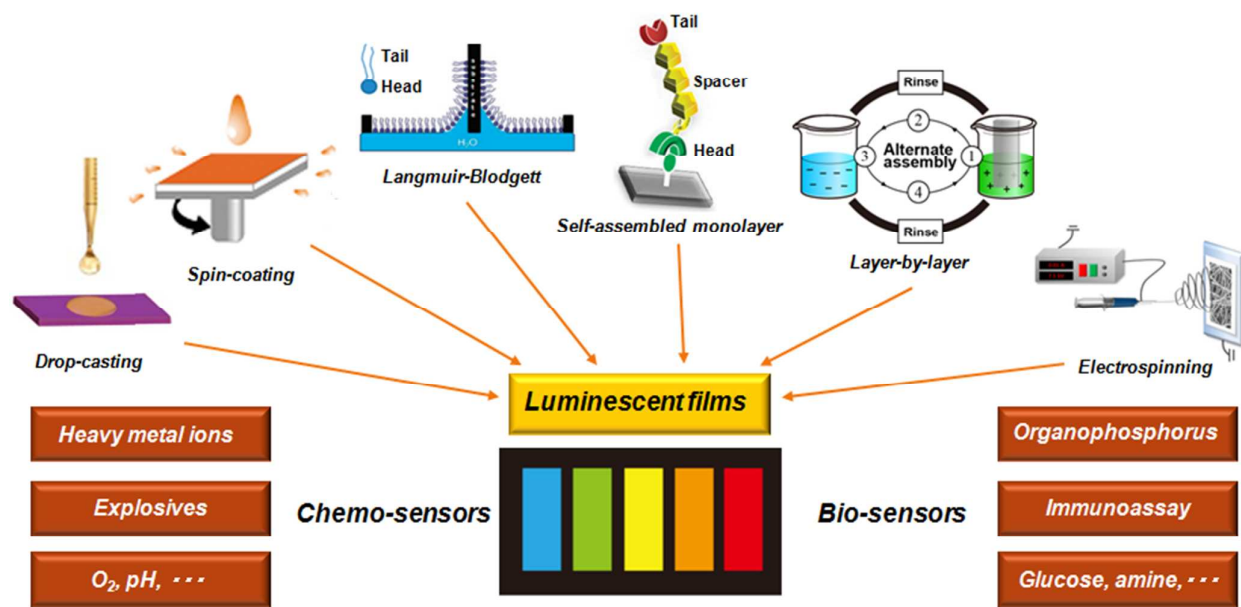


Fig. 1 Summary of the assembly methods of luminescent films for chemo-/bio-sensing applications.

emission molecule and some inorganic materials have been used to overcome this limitation. In addition, photostability of the films is the key parameter for their practical applications in the integrated sensor devices.

There are a variety of methods to fabricate luminescent films, and they mainly include drop-casting/spin-coating,^{50–52} Langmuir–Blodgett (LB) technique,^{53,54} self-assembled monolayers (SAMs) method,^{55–57} layer-by-layer (LBL) assembly,^{58–60} and electrospinning.^{61–63} Nowadays, there are a lot of reviews on solution-based luminescence probes^{2–6} or the fabrication methods of films.^{64–66} However, there are no comprehensive reviews on luminescent films for chemo-/bio-sensing. In this review, we will make such an effort to systematically review the progress of fabrication methods in designing various luminescent films for chemo-/bio-sensing (Fig. 1). We summarized the main methods for fabrication of luminescent film sensors, and demonstrated the sensing properties of such films that are related to their architecture. It is expected that this systematic review could be a guide to better understanding and fostering the design strategies of luminescent film sensors, and provide valuable clues for the fabrication of luminescent platform with sensitivity, selectivity, stability and portability.

2. Luminescent films *via* solvent evaporation method

2.1 Drop-/dip-casting

Solvent evaporation become the most popular technique for fabrication of luminescence thin-films due to its methodological simplicity and cost efficiency.^{67–69} Among the

solution-based processes, the drop-casting is the most extensively employed approach: a drop of compound solution is simply placed on a flat substrate, followed by drying in air or in an atmosphere of the solvent to evaporate off the solvent.^{70,71} In this process, the film architecture is relied on the self-assembly of molecules on the surface of substrate during the solvent evaporation. The solvent, the concentration of the solution, and the rate of the evaporation control the film morphology.^{72–74} Similarly, during the process of dip-coating, the substrate is immersed into the coating solutions, and then is withdrawn vertically followed by drying.^{75–77} The structure of films is closely related to the rates of evaporation and withdrawal speed of the substrate,⁷⁸ and, the film with smaller thickness is achieved by slower withdrawal speed.^{79–81} In general, in comparison to dip-coating, drop-casting technique is commonly used for the fabrication of luminescent film sensors.^{82–85} Therefore, we will concentrate on the applications of luminescent films in chemosensors by drop-casting technique.

2.1.1 Luminescent drop-/dip-cast film chemosensors for heavy metal ions

Heavy metal ions are of special concern due to their toxic effects and accumulated damage to biological systems. These species are non-degradable and tend to bio-accumulate in living organisms through the food chain, leading to serious debilitating illnesses. Monitoring of heavy metal ions in the environment is currently receiving considerable attention.^{86,87} As summarized in Table 1, luminescent sensors for many heavy metal ions with high sensitivity and selectivity are emerging in an endless stream.^{87–90} In general, a luminescent sensor was prepared in thin film for the rapid and portable detection of heavy metal ions.^{89,90} The commonly used fluorescent materials

for the sensing of metal ions include small organic molecules, conjugated polymers, QDs and noble metal NCs.

The sensitivity of luminescent measurement can be improved by photonic crystals (PCs), which are periodic dielectric structures marked “photonic band-gap”. The light propagation can be tuned with a certain wavelength through the Bragg reflection of PCs.^{91,92} When the light wavelength is in the range of the photonic stopband, the light will be reflected strongly by PCs. The PC-containing film could be fabricated by self-assembly of the fluorophore-labeled T-rich single stranded DNA (ssDNA) on the surface of Au-sputtered PCs. The single stranded chain of ssDNA would change to a folded hairpin structure in the presence of Hg^{2+} as a result of T– Hg^{2+} –T complexes formation. The decreased distance between the fluorophore and the thin gold film led to a fluorescence resonance energy transfer process, resulting in fluorescence quenching. Highly sensitive luminescent sensors with PC films have been developed for Hg^{2+} detection.⁹³ The detection limit of the sensor was calculated to be 4.0 nM, which was obviously enhanced compared to that of the control sample without PC structures (50 nM).

Recently, a hexaphenylsilole (HPS)-based photonic crystal (PC) film has been successfully used for the detection of Fe^{3+} and Hg^{2+} ions.⁹⁴ HPS-infiltrated PC film was fabricated by dripping HPS ethanol solution on the P(St-AM) PC films. The luminescence of HPS with aggregation-induced emission (AIE) properties was enhanced by PC. In the presence of metal ions, the electron-transfer from HPS molecules to metal ions led to the fluorescence quenching of HPS. The luminescent film exhibited high selectivity towards Fe^{3+} and Hg^{2+} owing to their high standard electrode potentials and small diameters. A linear relationship was found to exist between the expression $(1-F/F_0)$ and the concentrations of $\text{Fe}^{3+}/\text{Hg}^{2+}$ with a detection limit of 5 nM. Importantly, the response of the HPS-PC film sensor was reversible and reproducible by immersing in pure water after interacted with $\text{Fe}^{3+}/\text{Hg}^{2+}$.

Fluorescent turn-on probes possess reduced false-positive signals and the dark background. Therefore, they are superior to fluorescence quenching-based optical sensors. A “turn-on”

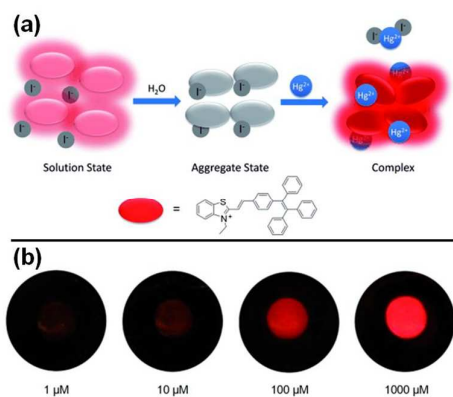


Fig. 2 (a) Schematic illustration of the mechanism for detecting Hg^{2+} . (b) Photographs of thin films of TPEBe-I containing different concentrations of Hg^{2+} (5.0 mL) in aqueous solution taken under 365 nm UV illumination. Reproduced from ref. 95. Copyright 2014 Wiley-VCH.

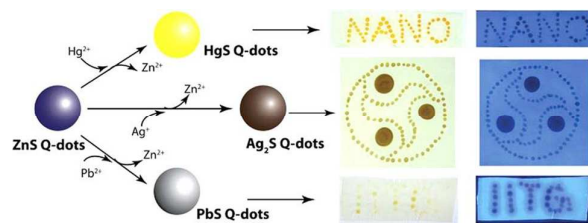


Fig. 3 Schematic diagram depicting the cation exchange mediated chemical transformation of ZnS QDs to HgS, Ag_2S , and PbS QDs along with the appearance of the drop cast of different metal ions onto the fabricated film under visible and UV light. Reproduced from ref. 97. Copyright 2012 American Chemical Society.

sensor with fluorescence turn-on response to Hg^{2+} has been designed based on AIE luminogens (Fig. 2).⁹⁵ Recently, Tang’s group designed a luminescent thin film by an AIE molecule, a tetraphenylethene (TPE)-functionalised benzothiazolium salt (TPEBe-X) with different counteranions exhibited tunable emission behavior from ACQ ($X = \Gamma$) to AIE (ClO_4^- and PF_6^-). The fabricated thin film of TPEBe-I appeared black under 365 nm UV irradiation, whereas strong red emission was observed in the case of TPEBe- ClO_4^- and TPEBe- PF_6^- films. Interestingly, the high affinity of Hg^{2+} toward Γ^- resulted in the removal of Γ^- from TPEBe-I in the presence of Hg^{2+} . The emission of TPEBe-I film was gradually enhanced with an increasing amount of Hg^{2+} . The detection limit of TPEBe-I film sensor was estimated to be 1.0 μM . Therefore, as a “light-up” fluorescent sensor, the TPEBe-I film sensor had higher sensitivity towards Hg^{2+} with high selectivity. Similarly, the fluorescence “turn-off/turn-on” for the Hg^{2+} based on the strong affinity of Hg^{2+} towards Γ^- was performed in conjugated polymer film.⁹⁶ Poly(1,4-bis-(8-(4-phenylthiazole-2-thiol)-octyloxy)-benzene) (PPT) acted as a new conjugated polymer was casted with polystyrene (PS) to fabricate a luminescent film. The fluorescence of such this film was turned off in the presence of Γ^- ions; however, this film displayed a “turn-on” response with the addition of Hg^{2+} ions. The proposed PPT- Γ^- luminescent film exhibited a selective and sensitive response towards Hg^{2+} with a detection limit of 1.6 μM .

Inorganic luminescent QDs have been also widely used for the design of fluorescent sensors due to their strong emission and excellent photostability.^{13,14} Recently, ZnS QDs were mixed with chitosan to devise a novel QD-based film sensor for the detection and removal of heavy metal ions.⁹⁷ The cation exchange took place between Zn^{2+} of ZnS QDs in the film and Hg^{2+} , Ag^+ and Pb^{2+} ions to produce the corresponding non-emissive HgS, Ag_2S , and PbS QDs (Fig. 3). Hg^{2+} , Ag^+ and Pb^{2+} could be distinguished under the visible light by yellow, dark, and light brown color, respectively. The visual detection limit of Ag^+ was determined to be 25 ppm and even to be lower (5 ppm) for Hg^{2+} and Pb^{2+} . In addition, the fabricated ZnS QD-chitosan film was able to remove the heavy metal ions. NCs have become powerful tools for luminescent sensing owing to their distinct advantages of low toxicity, prominent photostability and tunable fluorescent properties.^{17,98} Bovine serum albumin (BSA)-protected Au NCs have been

immobilized in a solid platform to fabricate reusable sensors of heavy metal ions.^{21,23,99} For instance, Zhang *et al.* developed a facile method of immobilizing BSA-Au NCs into polyelectrolytes to obtain the Au NCs-containing film for the detection of Cu²⁺.²¹ BSA-Au NCs, positively charged polydiallyldimethylammonium (PDDA) and negatively charged polystyrenesulfonate (PSS) were complexed and then drop-coated onto a glass substrate. The stable luminescent film can be effectively quenched by Cu²⁺ and Hg²⁺. More interestingly, Hg²⁺ can be masked by Sn²⁺, and thus this luminescent film displayed a linear correlation between the fluorescence intensity ratio F_0/F and the concentration of Cu²⁺ in the range of 100–500 μM . Furthermore, the quenched luminescence of the film sensor can be recovered upon immersing in EDTA solution to remove Cu²⁺ from the BSA-Au NCs, indicating the reproductive nature of the luminescent film.

Chi and co-workers have also described a recyclable Au NCs-based luminescent film for Cu²⁺ sensing.²³ They found that BSA itself possessed good film-forming ability under its isoelectric point without the aid of polyelectrolytes. Therefore, BSA-Au NCs could be directly drop-casted to form stable films with high adhesion. The red emission of BSA-Au NCs films can be significantly quenched by Cu²⁺ as a result of the strong chelation between Cu²⁺ and BSA. A linear correlation between the luminescence intensity and the concentration of Cu²⁺ was observed in the range of 30–500 μM with a detection limit of 0.5 μM . Importantly, the film sensors showed good selectivity towards Cu²⁺ over other metal ions. On the other hand, the quenched luminescence of this film can be recovered after the addition of histidine.

Different from the film deposited on the glass substrate, a free-standing composite film of Au NCs was prepared by dip-coating process using a parent chitosan film as a substrate.⁹⁹ The glutathione (GSH)-stabilized Au NCs were incorporated into the film *via* the combination of the amino group from chitosan with the carboxyl group from GSH. After exposure to aqueous Cu²⁺ solution, the luminescence of the film significantly decreased (Fig. 4). This can be attributed to the reduction of Cu²⁺ to Cu¹⁺/Cu⁰ by glutathione ligand or Au core of the cluster. The fabricated Au NCs film can detect

Cu²⁺ in the ppm range without interference by other metal ions such as Hg²⁺, As³⁺, and As⁵⁺. Moreover, the free-standing composite film was useful for practical applications as a portable device with high stability.

In comparison with the fluorescence probes at a single wavelength, ratiometric fluorescence sensors have increased sensitivity because the ratio of the fluorescent intensities at two wavelengths could provide a built-in correction.¹⁰⁰ On the other hand, the visualized detection can be achieved using ratiometric fluorescence sensors owing to the two-color interconversion.⁹⁰ Recently, based on nanohybrid of QDs and Au NCs, the ratiometric luminescent film has been successfully used for the visual determination of Pb²⁺.¹⁰¹ The red-emitting QDs were encapsulated into mercapto groups (–SH) functionalized silica nanoparticles. The green-emitting Au NCs were bonded to the QDs by the reaction between –SH and Au atoms. Then, the mixture of the QDs-Au NCs hybrid and poly(vinyl alcohol) (PVA) was dropped onto a glass slide to produce a ratiometric fluorescence film. The green luminescence of the Au NCs in the PVA film was quickly quenched in the presence of Pb²⁺. However, the red emission of QDs still remained constant, leading clearly visible luminescence color changes. The visual detection limit was 0.1 μM . In comparison to the single-fluorescence quenching method, the ratiometric luminescence sensor made Pb²⁺ easily noted by the naked eye. Furthermore, the excellent selectivity and high stability of the fabricated luminescent film allowed practical application in on-site determination of Pb²⁺ in real water samples.

2.1.2 Luminescent drop-/dip-cast film chemosensors for oxygen

Luminescent O₂ sensors have attracted much attention because of their potential applications in a variety of fields, including environmental monitoring, meteorology, and biology.¹⁰² Luminescent transition metal complexes, including cyclometalated Ru(II), Ir(III), and Pt(II) complexes, are regarded as promising candidates for photo-responsive molecular devices owing to their long-lived triplet excited state and the high quantum yield.^{103–105} The luminescent films for O₂ sensing are listed in Table 2. The unique excited-state properties of these materials allow them to be fabricated into luminescent films for sensing O₂ by quenching luminescence of transition metal complexes, owing to the energy transfer between luminescent transition metal complexes and the triplet ground state of molecular O₂.^{105–107}

The polymer films containing the luminescent transition-metal complexes can be simply fabricated by commonly used coating method. A great deal of reports have been focused on the development of novel luminescent transition-metal complexes to evaluate the O₂ sensing performances.^{108–111} The introduction of pyrenyl or pyrenylethynylene appendants into the Ru polypyridine complexes can significantly extend the life time of the Ru complexes. As a result, the detection sensitivity for O₂ can be improved. In polymer film, the quenching constant K_{SV} can be improved by 150-fold from 0.0023 Torr^{–1} to 0.35 Torr^{–1}.¹⁰⁹ In addition, the energy gap of Pt(II) complex was decreased by introducing electron-withdrawing or electron-donating groups. The Pt(II) complexes with low energy gaps are promising

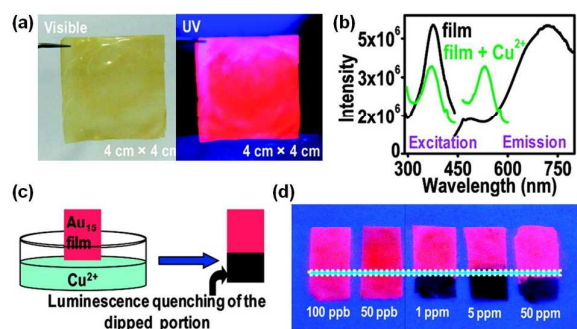


Fig. 4 (a) Photographs of the cluster incorporated film under white light and UV light. (b) PL spectra of the film before and after exposing to Cu²⁺. (c) Schematic diagram of the film sensor for the detection of Cu²⁺. (d) Dependence of Cu²⁺ concentration on luminescence quenching. Reproduced from ref. 99. Copyright 2012 American Chemical Society.

candidates for fabricating luminescent O₂ sensors with high sensitivity.^{110,111}

Usually, the probes for O₂ are excited by UV or visible light. Importantly, in order to make up the gap of NIR-excitabile sensors for O₂, Wolfbeis *et al.* used upconverting nanoparticles (UCNPs) as the excitation light source of an Ir(III) complex.¹¹ The UCNPs and the cyclometalated Ir(III) coumarin complex were incorporated in a gas-permeable polymer film. The fabricated film showed green to yellow luminescence (568 nm) excited by a 980 nm diode laser. In an atmosphere of O₂, the luminescence of Ir complex was obviously quenched, and the quenching constant K_{SV} was calculated to be 0.112%⁻¹.

More recently, Papkovsky's group has successfully developed a new luminescent O₂ sensor in polymeric film.^{113,114} Luminescent PtBP dye can be packaged in non-woven polyolefin materials with micro-porous structure for fabricating optical O₂ sensors by simple impregnation. The as-prepared sensors exhibited linear Stern–Volmer plots, and the lifetime changed with O₂ pressure (22–30 μs at 21 kPa and 50–60 μs at 0 kPa O₂).¹¹³ In addition, PtBP dye can be incorporated in polymeric materials by local solvent crazing.¹¹⁴ The sensors showed a linear O₂ calibration in the range of 0–100 kPa.

In fact, multifunctional sensors are required for practical applications. Dual fluorescence sensor for O₂ and temperature has been fabricated by dip-coating a fluorinated xerogel doped with both an O₂ probe and a temperature indicator.¹¹⁵ The dual sensor exhibited a linear Stern–Volmer plot for O₂ and had a good linear response to temperature in the 25–66 °C range independent of the O₂. The simultaneous sensing of temperature and O₂ has potential applications in various fields.

The O₂-sensitive colorimetric sensor can be fabricated to detect glucose by combining glucose oxidase with stable color background (green QDs layer).¹¹⁶ In the absence of glucose, the emission of O₂-sensing layer was quenched by O₂, and the sensor film represented green luminescence. In the presence of high concentrations of glucose, the O₂ was consumed during the glucose enzymatic reaction, and the emission of the sensor film was shifted to red. Therefore, the

glucose concentration could be directly readout through color change of the sensor. Furthermore, portable O₂ sensing device has been developed by using organic light-emitting diodes (OLEDs) as excitation sources.^{117,118}

2.1.3 Luminescent drop-/dip-cast film chemosensors for other analytes

It is well known that a better permeability of the film leads to a higher sensing efficiency. Moreover, the morphology of the film is of crucial for its permeability, which can be controlled through self-assembly.^{119,120} During the drop casting process, the self-assembly of oligoarene derivatives can be tuned by simply using different solvents, resulting different well-controllable organic nanostructures from the netted one-dimensional microbelts to the three-dimensional flowerlike supernanostructures (Fig. 5).¹¹⁹ The response speed of the three-dimensional flower-shaped supernanostructures for explosive (2,4,6-trinitrotoluene (TNT) and 2,4-dinitrotoluene (DNT)) vapors sensing is dramatically improved (700-fold) than that of one-dimensional microbelts. Takeuchi's group used a similar strategy to control the structure of the film sensors.¹²⁰ They designed a fluorescent charge transfer molecule and built the drop-cast films by tuning solvents. In the presence of chloroform, the film showed 12% fluorescence quenching exposed to DNT vapors for 10 min. In contrast, 91% fluorescence quenching of the film was observed upon the same treatment of DNT vapors using 1:3 (v/v) chloroform-toluene solvent.

Equal and smooth distribution of fluorescent compound on the substrate has a key role in determining the sensing efficiency of the luminescent film sensors. Recently, low-molecular-mass gelator with self-assembly properties was introduced for the fabrication of a network thin film by Fang's group.^{121,122} For example, the fluorescence-active compound CholG-3T-Py was dipped onto Chol-Ph-Chol-based molecular-gel films to fabricate uniform luminescent films with a rich network of structures. The activated film could selectively detect nitrobenzene (NB) owing to high vapor pressure of NB. In addition, the gel networks could also enrich the analyte onto the sensing layer of the film, resulting in the improvement of sensing performances.

In conclusion, these works illustrated the application of self-assembly for enhancing sensing efficiency of the luminescent film. However, the detection selectivity of the film sensors still remained a great challenge. In 2012, Burstyn *et al.* developed the carriers-impregnated luminescent films to improve the selectivity for ethylene sensing, such as silver(I) salts-impregnated luminescent films of poly(vinylphenylketone) (PVPK) or 1,4-bis(methylstyryl)benzene (BMSB).¹²³ In these films, Ag(I) salts and oligomer/polymer acted as the active sensing sites and the luminescent support as well as signal reporter, respectively. The luminescence quenching responses of the Ag(I)-impregnated films were only observed in the presence of gaseous analytes, which can form coordination bonds with the Ag(I) center, including C₂H₄, C₃H₆ and NH₃. Importantly, the oligomer/polymer support could also promote

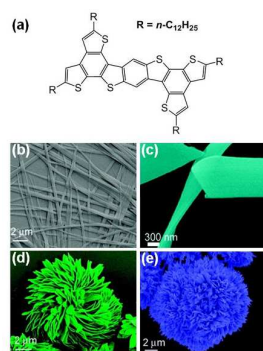


Fig. 5 Chemical structure of the oligoarene derivative and SEM images of different crystalline nanostructures. (a) Chemical structure of the oligoarene derivative; (b and c) Microbelt self-assembled from 1,4-dioxane; (d and e) Flower-shaped supernanostructures self-assembled from THF and n-decane solutions, respectively. All the three structures were self-assembled from 40 μL of solution with a concentration of 1 mg/mL through drop-casting onto glass substrates with a size of 1.5 × 2.5 cm². Reproduced from ref. 119. Copyright 2009 American Chemical Society.

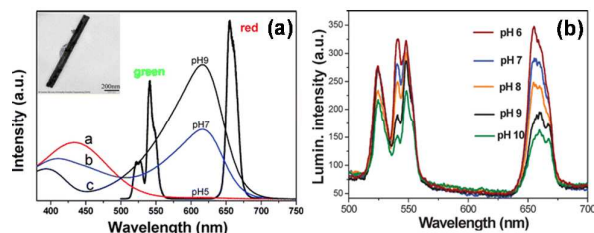


Fig. 6 (a) Absorption spectra of BTB in aqueous solutions of pH 5, 7 and 9, respectively (a, b, c); and luminescence emission (red and green) of the nanorods in cyclohexane solution following photo-excitation with a 980-nm laser. The inset shows a TEM image of the nanorods used. (b) Upconversion luminescence spectra of the sensor film as a function of pH upon diode laser excitation at 980 nm. Reproduced from ref. 131. Copyright 2009 The Royal Society of Chemistry.

the ion-pair separation of Ag(I) and thus improved the accessibility of the Ag(I) ion to the gaseous analytes.

Chow's group reported new heterobimetallic Ru(II)–Ln(III) donor-acceptor complexes for selective sensing of biogenic amine vapors by preferential coordination of amino functionalities to the metallic lanthanide.¹²⁴ Free-standing films were fabricated by blending the Ru(II)–Ln(III) submicrorods with polystyrene. The polymeric film exhibited an enhancement in luminescence after exposure to putrescine with a detection limit of 15 ppm. In addition, Wolfbeis's group found that chromogenic sensing of biogenic amines was achieved by using an amine-reactive chromogenic probe and an amine-insensitive fluorescein as a green emissive reference dye. The quantitative determination of biogenic amines can be simply achieved by the red-green-blue (RGB) readout of digital camera images.¹²⁵

The hydrophilicity of the film surface is essential for the sensing in aqueous solution. The sol-gel-based materials using tetraethylorthosilicate (TEOS) have been used to fabricate luminescent pH sensors.^{126,127} The dye-sol-gel films were prepared by dip-coating dye-doped sol-gel on glass slides. The hydrophilic character of the sol-gel can promote proton permeability in the film, and the TEOS precursor can improve the adhesion stability of the films. Moreover, the microstructure of the matrix can be tailored to completely encapsulate the dye, resulting in high pH sensing performances (Table 3). The pH-sensitive fluorescent dye (*e.g.*, pyranine) can also be used for the detection of CO₂.¹²⁸ The hybrid xerogels film by dip-coating exhibited a linear response to CO₂ in the range 0–30%, and the limit of detection for CO₂ was calculated to be 0.03%. On the other hand, the incorporation of a phase-transfer agent and the covalent immobilization of the pH-indicator on the polymer chains could improve the sensitivity and stability of the sensors.¹²⁹

In order to eliminate the background absorption and autofluorescence, upconverting nanorods and longwave absorbing pH probes were incorporated together into the pH-sensitive films.^{130,131} The absorption spectra of the pH-sensitive dye partially overlap the visible emission of the UCNP. The deprotonated form of BTB absorbs and exerts a strong inner filter effect on the emission of the nanorods. At low pH, BTB has no insignificant absorbance in the emission range of the

nanorods (Fig. 6). In the pH range 6–10, the sensor film showed fast (< 30s) and reversible responses to pHs. Furthermore, this kind of pH sensor can also be used for sensing acidic gases (CO₂) or basic gases (NH₃).^{132,133} Based on the similar principle, UCNP have also been applied for glucose sensing using fluorescein derivative-labelled enzyme glucose oxidase and flavin adenine dinucleotide. In the presence of glucose, the concentration of O₂ was decreased. Thus, reduction state of flavin adenine dinucleotide had weak absorbance in the emission range of UCNP. As a result, the fluorescence of fluorescein derivative excited by UCNP increased with increasing glucose concentration.¹³⁴

However, the single-channel sensors usually have the limitation of a low signal-to-noise ratio. Qin *et al.* reported a ratiometric pH sensor based on upconverting nanorods and pH probe ETH 5418.¹³⁵ The absorbance of protonated and unprotonated ETH 5418 overlap the green emission and red emission of the upconverting nanorods, respectively. When the pH of the sample changed from 6 to 11, the sensor film exhibited the decreased green emission and the increased red emission. More recently, color-switching pH sensor using poly(*N*-phenylmaleimide) (PPMI)-containing block copolymer has been developed.¹³⁶ Ratiometric tricolor switching behavior was observed for the PPMI polymer in an almost entire pH range. Unique self-assembled morphology of the PPMI-containing block copolymer can eliminate uncontrolled aggregation.

In addition, the group of Zang developed the ratiometric luminescent film to sense vapor of H₂O₂ at trace levels *via* Förster resonance energy transfer (FRET) between the pristine and reacted sensor molecules (Fig. 7).¹³⁷ A fluorescence molecule containing aryl boronate group (DAT-B, 500 nm) could selectively react with H₂O₂, producing an electronic “push-pull” structure DAT-N, which had a red-shifted emission wavelength (574 nm). The spectra overlap between the donor (DAT-B) emission and acceptor (DAT-N) absorption enabled the efficient FRET to produce high sensing efficiency. Moreover, the short distance between the molecules in the solid film can promote the occurrence of FRET between DAT-B and DAT-N. The detection limit of DAT-B luminescent film for H₂O₂ vapor was calculated to be 7.7 ppb.

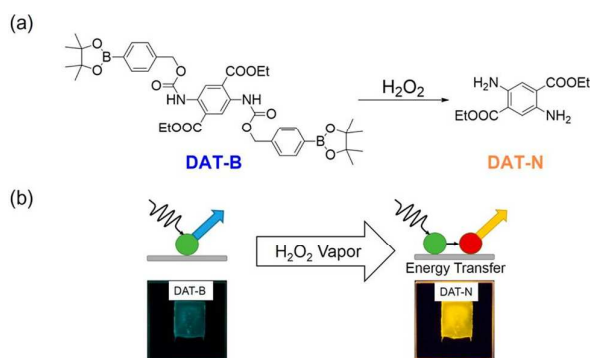


Fig. 7 (a) Chemical reaction between the sensor molecule (DAT-B) and H₂O₂, leading to the formation of DAT-N. (b) Illustration showing the intrinsic fluorescence emission of DAT-B and the FRET process between DAT-B and DAT-N. Reproduced from ref. 137. Copyright 2014 American Chemical Society.

Through the addition of an organic base to accelerate the oxidation of aryl boronates, the fast response time (less than 0.5 s) was observed upon exposure to 1 ppm of H₂O₂ vapor. In addition, they found that the sensitivity can be further enhanced by spin-coating the sensor material into an optical tube connected to a photodetector.

In conclusion, the drop-/dip-casting method has been extensively used for luminescent films owing to its very facile operation and general applicability. However, this method suffers from some inborn weaknesses (*e.g.*, poor uniformity). On the other hand, ACQ effect is usually occurred in the traditional fluorescent molecules, conjugated polymers and QDs. In addition, blending polymer is not mandatory, but helpful for an enhancement of adhesion. The sensing performances of the polymer film are significantly influenced by diffusion rate of analytes. Therefore, the polymer with good permeability should be the first choice.

2.2 Spin-coating

The spin-coating technique is expected to be applicable for the fabrication of a variety of thin-film based devices.^{138,139} In the spin-coating deposition, a drop of the solution is placed on a substrate, the solution is rapidly spread over the surface and the excess coating will be spun out of the edge of the substrate by centrifugal force. A residue on the substrate remains to rapidly form a thin-film by solvent evaporation. In addition, multi-layer films may be fabricated by repeating the above process.^{140–142} The thickness of spin-cast film can be controlled by altering the spin speed and the concentrations of the cast solutions.^{143–145} In comparison to drop/dip-casting technique, the spin-coating process is adapted to fabricate the thicker and multiple layers with high uniformity.^{146,147} In general, polymers are widely used as materials for spin-coat film owing to the superior film-forming characteristics and the ability to incorporate multiple functions in the film design.¹⁴⁸

2.2.1 Luminescent spin-coat film chemosensors for explosives

Explosive compounds, mainly composed of nitro-organics, nitramines and peroxides, are dangerous chemical agents and chemical warfare agents. The trace detection of explosives and explosives-related compounds has received widespread attention in national defense, public security, environmental cleaning and human health.^{149,150} Nitroaromatic explosives, such as TNT, DNT, nitrobenzene (NB) and picric acid (PA), are widely employed in industrial explosives.^{151,152} Nitroaromatic explosives have a moderate vapour pressure that can be detected by solid-state sensor platform in vapor phase.¹¹⁷ The list of luminescent films for explosives sensing are shown in Table 4. The main principle for their fluorescent detection is based on the formation of π -stacking complexes between electron-deficient nitroaromatics and electron-rich fluorophores, leading to the luminescence quenching.¹⁵³

Fluorescent conjugated polymers in luminescence sensing have intrinsic ability to amplify the response to the analyte-binding event expressed as “superquenching effect”, and they have commonly used for the detection of explosives.¹⁵⁴ An

early example of spin-cast polymer fluorescent film for nitroaromatics was found using polyacetylene, poly[1-phenyl-2-(4-trimethylsilylphenyl)ethyne] (PTMSDPA) with exceptionally high permeability and large free volume.¹⁵⁵ The formation of charge-transfer complex between electron-rich PTMSDPA and electron-poor nitroaromatics resulted in luminescence quenching of the film. Importantly, the sensing rate of PTMSDPA film increased with a decrease in the thickness (from 80 nm to 3 nm) of the film owing to the higher vapor permeability of PTMSDPA in a thinner film.

However, most of the conjugated polymer systems were planar conjugated, leading to a decreased fluorescence quantum yield in the solid states. To prevent the π -stacking of the polymer backbones, Swager's group revolutionarily incorporated three-dimensional pentaptycene moieties into conjugated phenyleneethynylene polymers.^{156,157} The synthesized pentaptycene-derived conjugated polymers were spin-casted to fabricate high efficient and stable luminescent films. Upon exposure to TNT and DNT vapors, these films suffered luminescence quenching by electron-transfer from the excited polymers to the analytes. Moreover, the diffusion of analytes was accelerated in the sensor film by the formation of cavities between adjacent three-dimensional polymers. The luminescence properties of conjugated polymer films could be improved by the combination of pentaptycene and TPE units.¹⁵⁸ Two main advantages were obtained for this kind of luminescent film: the three-dimensional pentaptycene with rigid structure could prevent π -stacking and the TPE possessed AIE effect to improve luminescence. The fabricated luminescent

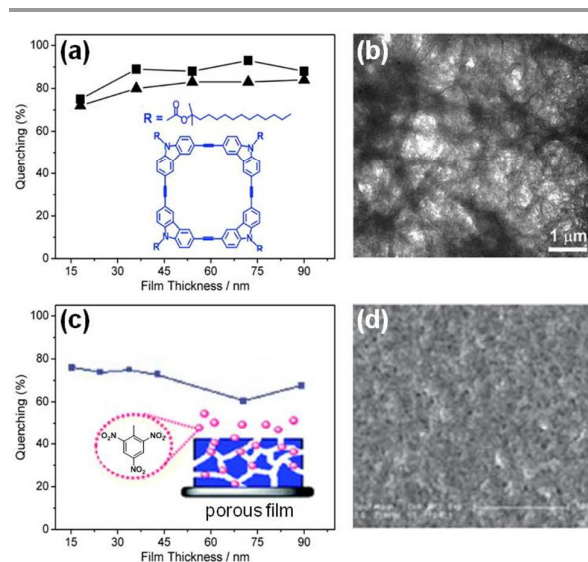


Fig. 8 (a) Thickness dependence of fluorescence quenching efficiency of ACTC film upon exposure to saturated vapor of TNT (▲) and DNT (■) for 60 s. (b) TEM image of a thin film of ACTC cast on silicon oxide from 2 mM THF solution. Reproduced from ref. 160. Copyright 2009 American Chemical Society. (c) Thickness dependence of fluorescence quenching efficiency of P1 film prepared from its toluene solution upon exposure of the film to a saturated vapor of TNT for 60 s. (d) SEM of the P1 film by spin-casting from its toluene solution. Reproduced from ref. 166. Copyright 2013 The Royal Society of Chemistry.

films were utilized to detect the electron-deficient isocyanates by electron-transfer mechanism. 74% fluorescent signal was quenched within 60 s. The detection limit was at the ppt level, which was substantially lower than their permissible exposure limit of 5 ppb.

Ultrathin thickness for the above rigid films is still required for high quenching efficiency even in the case of conjugated polymers with three-dimensional pentaptycene. However, porous films composed of molecular nanofibers or gelators were emerged to achieve satisfactory quenching efficiency regardless of the film thickness. In addition, porous films have large surface areas so as to promote the diffusion of analytes to sensing elements and strengthen the interaction between analyte molecules and sensing sites.¹⁵⁹ An alkoxy-carbonyl-substituted carbazole-cornered conjugate tetracycle molecule (ACTC) was synthesized and spin-casted to form luminescent porous film sensors by the group of Zang.^{160–162} The rigid in-plane conjugated structure of ACTC enabled the cofacial π - π stacking between the molecules to produce one-dimensional nanofibril structures. The nanofibril films were obtained by spin-casting a THF solution of ACTC. When the ACTC films were exposed to TNT and DNT vapors, the efficient fluorescence was quenched by electron-transfer from the excited ACTC to the explosives. Thanks to the porous structures, the nanofibril films exhibited thickness-independent luminescence response to TNT and DNT vapors with high stability and reproducibility for the practical application (Fig. 8).

Some other molecules (*e.g.*, carbazole and pyrene derivatives) can also form molecular nanofibers in spin-casted films.^{163–165} For instance, phosphonated pyrene derivatives have been developed to fabricate porous and fibril-structure films for nitroaromatic explosives sensing.¹⁶⁴ The P=O moieties are capable of decreasing the lowest unoccupied molecular orbital (LUMO) energy of molecules, facilitating electron-transfer from electron rich pyrene to electron deficient nitroaromatic compounds. Moreover, the sensitivity could be further enhanced by a closer contact, resulting from hydrogen bonding interactions between the phosphonic acid and the nitro groups of nitroaromatics. On the other hand, the formation of π - π stacking between pyrene and polyethersulfone in the polymer films can improve the sensing performances.¹⁶⁵ Interestingly, the spin-coated luminescent film of pyrene-PES possessed a worm-like structure, leading to improved diffusion rate of TNT vapor and consequently improved the detection sensitivity. In addition, Xu and co-workers developed a porous sensing film fabricated from a conjugated polymer gelator **P1** by drop-/spin-coating its toluene solution.¹⁶⁶ As shown in Fig. 8, the porous morphology was beneficial for the diffusion of gaseous analytes, allowing effective detection of TNT vapor with a little dependent on film thickness. In comparison to the polymeric gelators, the gelation behavior of the dendritic gelators can be promoted *via* multiple non-covalent interactions. Han *et al.* designed a carbazole-based conjugated dendrimer H2-BCz with selective gelation behavior in a good solvent and anti-solvent mixture.¹⁶⁷ Xerogel film with the nanofibers was obtained by spin-coating the H2-BCz gel on a quartz slide. The xerogel films can be used as chemsensors for the detection of

nitroaromatics due to the electron-donating property of the H2-BCz molecule. In conclusion, the molecular nanofibers or gelators are suitable for spin-casting porous film, however, the difficulty in design and synthesis reduces their versatility.

Combination with the casting techniques, sol-gel method has also been used to build porous film sensors with enhanced efficiency.¹⁶⁸ Silica sol-gel matrices offer the enticing prospect in this regard owing to their unique and fascinating properties (tunable porosity, chemical inertness, thermal stability, facile surface modification) and well-established ability to maintain activity and stability of the incorporated sensory elements in the films.^{169,170} For example, metalloporphyrins serving as sensing unit were incorporated in mesoporous silica films using surfactants as structure-directing agents.¹⁷¹ The fabricated cadmium porphyrin (CdTPP)-doped bicontinuous worm-like film showed high quenching efficiency towards TNT (60% quenching after 10 s exposure to TNT vapor). Not only the mesostructure of the film, but also strong affinity between analytes and sensing elements provided a fast response time. Similarly, a fluorophore-doped mesoporous silica film was designed using pyrene based fluorophores TKMPP.¹⁷² The inclusion of surfactant in the surfactant-containing TKMPP-doped film with worm-like architecture improved the binding interaction between fluorophore and DNT, resulting in an enhanced quenching performance towards DNT vapor (39% quenching after 45 s and 94% after 405 s) with a detection limit of 10 nM. In addition, the silica framework could protect the fluorophores from their undesirable photobleaching, leading to the long-term storage stability of the nanocomposite films.

Additionally, organically modified silica (ormosil) was utilized to prepare the porous film *via* a facile template-free sol-gel method in the absence of additives (*e.g.*, surfactants).¹⁷³ Fluorescent pyrene molecules were physically encapsulated in the ormosil network during the synthesis. The mesoporous ormosil can promote the formation of pyrene excimer in the thin film, leading to an enhanced emission. The as-prepared film exhibited rapid luminescence quenching response against electron-deficient TNT, DNT and NB vapors. Other organic gases, such as toluene and benzene, had no interference on the

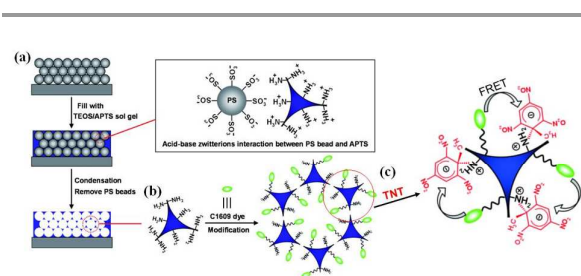


Fig. 9 Schematic illustrations for (a) the fabrication of inverted opal silica film with amino ligand monolayer at porous surface; (b) further modification with dye molecules through the covalently linking reaction between amino groups and C1609 dye; (c) schematic illustration for the FRET-based inverted opal sensors for TNT detection and fluorescent quenching mechanism through resonance energy transfer from C1609 dye donor to TNT-amine complex acceptor. Reproduced from ref. 174. Copyright 2009 Wiley-VCH.

detection, indicating good selectivity of the film sensor towards nitroaromatic compounds. Furthermore, the quenched luminescence of the film can be recovered by simply washing the films with water.

Different from the amorphous silica films mentioned above, an inverted opal silica film with ordered porous structure was also developed for the detection of nitroaromatic explosive.¹⁷⁴ At first, a three-dimensional-ordered photonic crystal film on a silicon substrate was fabricated using sulfonic groups modified PS microspheres *via* solvent evaporation, followed by padding with a mixed tetraethylorthosilicate/3-aminopropyltriethoxysilane (TEOS/APTS) sol-gel. Subsequently, the inverted opal SiO₂ film with the amino ligand layer at the interior surface was obtained after the PS template was removed. Finally, C1609 dye was covalently immobilized to the partial amino ligands on the interior surface of porous walls (Fig. 9). The film exhibited a selective quenching response towards TNT as a result of the non-emissive resonance energy transfer from dye donors to TNT-amine complexes. The highly ordered porous structure and strong analyte affinity allowed the film to be capable of detecting TNT vapor in the low ppb levels.

In order to improve the sensitivity towards nitroaromatic explosives, a lasing action in organic polymers has been used in hybrid films composed of a conjugated polymer and titania (TiO₂) nanoparticle.¹⁷⁵ The conjugated polymers functioned as both the gain medium and the sensory unit. The nanosized TiO₂ endowed the hybrid film with a random lasing action. This strong lasing suffered significant attenuation in the presence of trace TNT (10 ppb). The sensitivity to TNT vapor was 20 times higher than that observed from spontaneous emission. The developed concept could expand to achieve ultra-sensitive trace analysis in general domains by incorporating the other functional materials other than the conjugated polymer.

The conjugated polymer-based materials possess high chemosensory efficiency for the detection of electron-deficient nitroaromatics *via* the electron-transfer mechanism; however, it remains a challenge to effectively improve the selectivity towards a

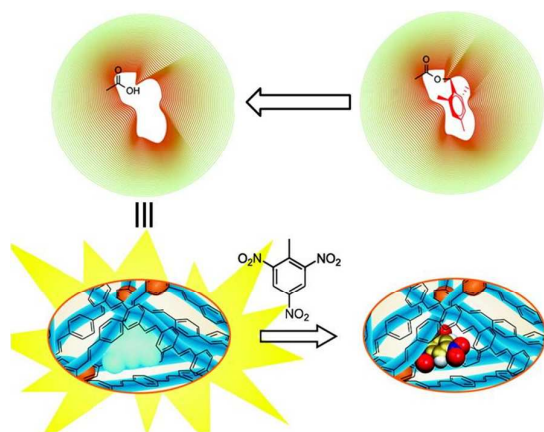


Fig. 10 Schematic representation of a template imprinted into a CP network and TNT sensing. Reproduced from ref. 176. Copyright 2007 American Chemical Society.

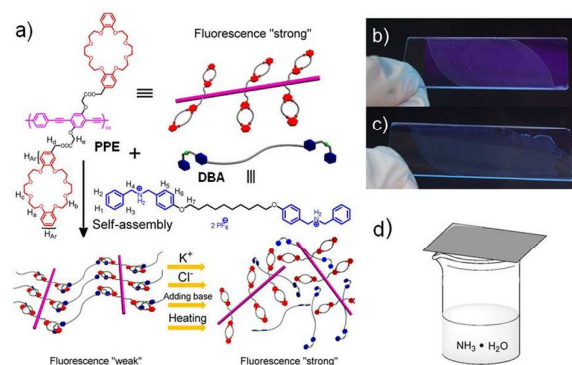


Fig. 11 (a) Cartoon representation of the formation of a supramolecular cross-linked conjugated polymer network and its disassembly induced by different signals. (b) Photograph of a film of PPE polymer, illuminated at 365 nm. (c) Photograph of a film of a mixture of PPE and DBA with a molar ratio of 1:10, illuminated at 365 nm. (e) Cartoon representation of exposure of a film made from the supramolecular network to ammonia. Reproduced from ref. 181. Copyright 2012 American Chemical Society.

specific molecule. The introduction of molecular imprinting technique in the fabrication of film sensors provides an effective way to obtain selective sensors for a particular analyte. Nesterov and co-workers designed highly selective luminescent chemosensors based on molecularly imprinted conjugated polymer materials (Fig. 10).¹⁷⁶ The conjugated polymers acted as both imprinting materials and analytical signal transducers. The “TNT imprinted” polymer spin-coat film was capable of selectively detecting TNT by the shape/size recognition. However, stronger fluorescence quenching was unexpectedly observed on exposure to DNT vapor as a result of the similarity between TNT’s and DNT’s molecular shapes. The specificity toward TNT molecules could be improved by choosing a surrogate template, which fairly well matched the TNT molecular shape.

2.2.2 Luminescent spin-coat film chemosensors for other analytes

During the past decades, gas sensors are of significances for toxic or harmful gases and monitoring of air quality,^{177–179} and thus spin-coat luminescent films with controlled thickness and morphology have also proven to be suitable for other gases sensing.^{180,181} For instance, fluorine-thiophene-based luminescent spin-coat films were developed for the detection of methamphetamine (MA) vapor.¹⁸⁰ 9,9-dioctylfluorene-2,7-bisthiophene (FBT) and poly[(9,9-dioctylfluorenyl-2,7-diyl)-alt(3-hexylthiophene-2,5-diyl)] (PFT) were used to fabricate the two films. The imine group of MA molecule can reduce heavy atom effect of thiophene and its phenyl can form π - π stacking with FBT or PFT. The prepared two films revealed luminescence enhancement upon exposure to MA vapors in sealed vials. In comparison to the PFT film, the FBT film had higher sensitivity towards MA because its thiophene content was higher, providing more binding sites to MA. The detection limits for MA vapor of FBT and PFT are 1.9 ppm and 6.4 ppm. In addition, a multiple fluorescent sensor based on supramolecular cross-linked conjugated polymer network was reported by

Huang *et al.* (Fig. 11).¹⁸¹ The network was constructed by mixing dibenzylammonium salt (DBA) cross-linker with fluorescent conjugated polymer poly(phenylene-ethynylene) (PPE) containing pendent dibenzo[24]crown-8 (DB24C8) group. A luminescent film of the supramolecular cross-linked network was obtained by spin-casting the mixture onto glass slide. The fluorescence of the fabricated film was relatively weak as a result of the host-guest interactions between DB24C8 and DBA, inducing the self-assembly of PPE and the aggregation of polymer chains. However, the complexation of DB24C8 and DBA were destroyed by multiple stimuli, such as potassium cation, chloride anion, pH increase, and heating. Therefore, the transformation of supramolecular crosslinked network into linear polymer led to an increase of luminescence intensity. Finally, this film has been successfully used for the detection of ammonia with satisfactory results.

The spin-coat films own robust architecture and high stability and thus they have also been used for detecting analytes in solution.¹⁸²⁻¹⁸⁴ For example, Jiang and co-workers reported a copolymer film sensor for HSO_4^- with a turn-on fluorescence.¹⁸² The imine and adjacent hydroxymethyl groups in poly(HEMA-co-VNP) were capable of forming multiple hydrogen bonds with HSO_4^- anion. The intramolecular excimer was generated from neighbouring side and the emission occurred. Therefore, hydrophilic copolymer poly(HEMA-co-VNP) in this thin film showed a red shifted emission at about 450 nm upon HSO_4^- both in organic and aqueous media. On the other hand, the fluorescence displayed a linear enhancement on HSO_4^- concentration in the range of 0–160 μM with a detection limit of 50 μM . Importantly, the turn-on fluorescence response can be easily distinguished by the naked eye.

For sensing ions in aqueous solution, good hydrophilicity of the film sensors is essential to improve the permeability of ions into the film, and thus hydrophilic copolymer containing the ion-sensitive fluorescent unit can be utilized to build hydrophilic polymeric films.¹⁸³ hydrophilic copolymer poly(HEMA-co-DCPDP) was obtained by incorporating the Cu^{2+} -sensitive DCPDP (fluorescent unit) and the 2-hydroxyethyl methacrylate (hydrophilic unit) together. Cu^{2+} ions caused a significant decrease in fluorescence intensity of the spin-coated copolymer with high selectivity and sensitivity. Meanwhile, a turn-on fluorescence at about 590 nm was observed after the Cu^{2+} -treated film was immersed in the solution of $\text{P}_2\text{O}_7^{4-}$. In addition, this polymer film showed high stability in the flowing water, and thus it can be potentially used for the online monitoring in a continuous bioprocessing.

Zeng and co-workers reported a FRET-based ratiometric sensor for Hg^{2+} by depositing the functional layers (donor, spacer, and acceptor) on a sol-gel silica support layer.³⁵ In the FRET system, the nitrobenzoxadiazolyl derivative (NBD) acted as the donor and the non-emissive spiro lactam rhodamine B (SRhB) functioned as the receptor for Hg^{2+} ions. Hg^{2+} -triggered ring-opening of SRhB can produce emissive RhB. As a result, the NBD emission at 528 nm decreased and the RhB emission at 588 nm appeared owing to the occurrence of the energy transfer between NBD and RhB. A linear correlation was

observed between the ratio of the fluorescence intensities F_{588}/F_{528} and the concentration of Hg^{2+} in the 1.0–10 μM range with a detection limit of 1.0 μM . The solid luminescent film was suitable for visible detection for Hg^{2+} ; however, it is still a great challenge to select suitable donors and receptor for the design of FRET system. Fortunately, an internal reference was used for the ratiometric detection of Hg^{2+} , avoiding the use of FRET.¹⁸⁴ In the proposed system, BSA-Au NCs were incorporated in a sol-gel-derived mesoporous silica film for the selective and sensitive ratiometric detection of Hg^{2+} by exploiting the luminescence signal at 420 nm arising from oxidized BSA as an internal reference. The detection limit for Hg^{2+} was calculated to be as low as 0.6 nM.

In biological samples, the interfering absorption and autofluorescence of biological matter would influence the UV or blue range of the fluorescence spectra. One way to overcome these issues is to use near infra-red fluorescent pH sensing film.^{185,186} A long wavelength fluorescent hydrophilic copolymer containing the pH-sensitive chromophore naphthalenediimide has been synthesized as pH sensor.¹⁸⁶ The spin-cast film of the obtained hydrophilic copolymer exhibited a sensitive and linear response towards pH in the range of 4.6–8.0. The interferences from biological samples can be minimized by the long excitation wavelength at the isosbestic point of 572 nm and long wavelength emission at 630 nm. Furthermore, in order to eliminate the autofluorescence, UCNP s have been chosen as the light source, and the luminescence spectra of UCNP s have been modulated by the pH indicator dye.¹⁸⁷ The as-prepared film exhibited a ratiometric fluorescence response to pH because the absorption of pH indicator is higher at 661 nm than that at 671 nm. Finally, if the sensor film was implanted beneath 6–7 mm of porcine tissue, the calibration curve remained unchanged, indicating the great potential in vivo sensing.

Most of the above-mentioned methods to construct film sensors *via* a spin-coating technique enjoy key advantages of generality and uniformity. However, the spin-coating technique suffers from certain drawbacks (*e.g.*, the lack of material efficiency).¹⁸⁸⁻¹⁹⁰ In principle, all of the luminescent materials can be used for spin-coating. Unfortunately, fluorescence quenching by ACQ effect also exists in this technique. The utilization of AIE materials and three-dimensional conjugated polymers could avoid the ACQ effect. Another possible solution is to use the micro-/nanosized particles by incorporating the probes in a proper polymer host. Moreover, the precursor solution should own appropriate viscosity for the formation of films. Therefore, the polymer is of crucial importance for spin-coating. In comparison with drop-casting, it is uneasy to deliver an exact amount of particles onto a substrate.

3. Luminescent films *via* Langmuir–Blodgett (LB) technique

As the first molecular-scale material technique, LB technology has been employed in monolayer film fabrication, in which the interfacial properties are tailored at the molecular level.¹⁹¹ The

LB technique is based on the formation of a Langmuir monolayer on water, when amphiphilic molecules orient themselves at the air/water interface.^{192–195} The ordered and oriented monolayer films with high surface pressures can be transferred to solid substrates to form LB films. In addition, multilayers can be fabricated by repeating the LB process for desired times with different types of LB deposition.^{192,193} In recent years, a series of materials, such as amphiphilic compounds, transition-metal complexes, nanoparticles and biomolecules, have been proposed as candidates to construct the luminescence-based LB films for chemo-/bio-sensing applications.

3.1 Luminescent LB film chemosensors

LB luminescent film is sufficiently sensitive to determine various gaseous analytes owing to its thin single-layered structure and high specific surface. In principle, gas sensing of luminescent LB film is based on the quenching of immobilized luminophors in the ambience of target gas.^{196–199} For instance, LB films of transition metal complexes have been used to detect O₂ through a fluorescence quenching mechanism. Amphipathic transition metal complexes were synthesized by ligands-functionalization, and a sensitive single-layered O₂-sensing LB film was fabricated by using ligands-functionalized ruthenium(II) bipyridyl complexes (Fig. 11).¹⁹⁶ The luminescence response of the films was observed rapid and reversible when the ratio of O₂ was switched from 0% to 100% as a result of the high absorption capability of O₂ molecules on the complexes. Nonlinear Stern-Volmer plots are explained by the two-site model or nonlinear solubility model.

In general, the self-quenching of the complexes often occurs during the LB process. Recently, the group of Sato introduced the inorganic host materials (clay mineral) to prevent the self-quenching of the complexes.^{197–199} In 2011, an inorganic-organic hybrid LB film was constructed by host-guest interaction between clay and an iridium(III) complex.¹⁹⁷ A floating hybrid film was formed on a subphase of an aqueous dispersion of clays, followed by transferring onto a hydrophilic glass or silicon substrate. The luminescence intensity of the film exhibited rapid decrease within 2 s upon exposure to gaseous O₂. Meanwhile, the quenched luminescence can be recovered to the initial value within 5 s in the absence of O₂ gas. In comparison with the polymer film of iridium (III) complex, the ultra-thin LB film (8–16 nm) requires less complex materials and responds more rapidly to gaseous O₂. Subsequently, they also fabricated dual emitting LB multilayered film for sensing O₂, which composed of clay and two kinds of iridium (III) complexes.¹⁹⁸ In addition, the other organic gases (*e.g.*, methanol, pyridine and acetone) have been detected by the LB film of iridium (III) complexes, although the mechanism of the introduced gas-induced fluorescence quenching was unclear.¹⁹⁹

Peptide lipids have been applied to establish several LB films for sensing metal ions due to the unique binding affinity between peptide lipids and metal ion at air-water interface.⁵³ As shown in Fig. 12, the ionophore and the fluorophore were co-

existed in lipid **A** (Dns–Gly–His–Lys–(C₁₈)), which was next used to construct a LB luminescent film. The fluorescence of the LB film of lipid **A** was quenched in the presence of Cu²⁺ by intramolecular ionophore-fluorophore coupling. For the mixed monolayer LB film, the ionophore and the fluorophore were located on lipid **B** (Gly–His–Lys(C₁₈)) and lipid **C** (Dns–Lys(C₁₈)), respectively. The fluorescence of this mixed LB film was quenched in the presence of Cu²⁺ by the through-space interaction mechanism. In addition, the quenched fluorescence can be effectively restored after treatment with HCl. The LB luminescent films fabricated by the mixture of lipid **B** with the other fluorescent lipids (*e.g.*, fluorescein lipid) also exhibited the excellent quenching properties towards Cu²⁺, indicating the potential of the intermolecular receptor-fluorophore interaction mechanism in luminescent sensing.

Water-soluble conjugated polymers have been widely used as sensory materials for inorganic ions and organic small molecules.^{10,11} However, the conjugated polyelectrolyte-based sensors are often disturbed by ionic strength and charged molecules in solutions. Swager's group immobilized hydrophobic, water insoluble poly(*p*-phenylene ethynylene)s (PPEs) poly(*p*-phenylene ethynylene)s (PPEs) in the LB film for the detection of viologens in the aqueous solution.²⁰⁰ The tight and ordered localization of polymer molecule can facilitate the exciton transport in multiple dimensions, leading to the increased sensitivity to viologen in comparison with polymer solutions. In addition, the hydrophobic surface of the LB film can promote the interaction between the hydrophobic groups of viologens and PPEs. The proposed system provided a strategy to establish the solid-state sensory devices for monitoring organic small molecules in aqueous environments.

3.2 Luminescent LB film biosensors

It is one of the leading sectors of applications in the biosensing field to design and develop nanostructured sensors. The molecular-scale LB technique has been proposed for the preparation of biosensors using bioactive molecules (*e.g.*, antibodies and enzymes) as the biorecognition elements (Table 5).^{201,202}

An enzyme-based sensor not only provides high selectivity, but also works in an environmentally friendly way. Enzyme can

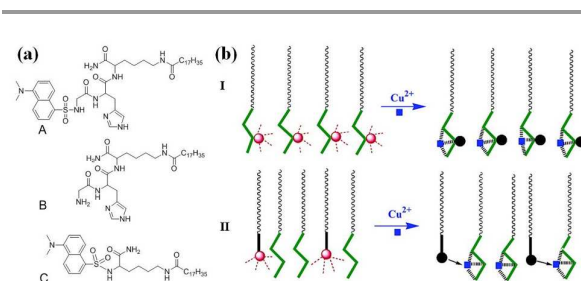


Fig. 12 (a) Structures of lipid **A**, **B** and **C**. (b) Proposed mechanisms on the fluorescence quenching of langmuir monolayers caused by copper ions. **I** shows the intramolecular scheme for the monolayer of lipid **A**. **II** shows the intermolecular scheme for monolayers of **B/C**. Reproduced from ref. 53. Copyright 2003 American Chemical Society.

be adequately immobilized in an organized ultra-thin monolayer while its biological activities were retained. LB monolayer of FITC-labeled enzyme organophosphorus acid anhydrolase (OPAA) was prepared for the detection of diisopropylfluorophosphate (DFP).²⁰³ OPAA rearranged during the enzymic hydrolysis of DFP, leading to self-quenching of FITC fluorescence in the FITC-OPAA film. A linear relationship was observed between the emission intensity of the film and the concentration of DFP in the range of 1.0–10 nM. Interestingly, the enzyme in the LB film can return to its original configuration when placed in the buffer solution so that the fluorescence of the film can be fully recovered. The same research group also immobilized FITC-labeled organophosphorus hydrolase (OPH) in the LB film to construct a paraoxon sensor.²⁰⁴ Different from the LB film of FITC-OPAA, the fluorescence quenching of this FITC-OPH film sensor in the presence of paraoxon is caused by tuning the pH values during the hydrolysis reaction. With an increase in the paraoxon concentration from 0.1 to 10 μM , the fluorescence of FITC-OPH film decreased linearly with a detection limit of 1.0 nM.

In addition, Kim and co-workers designed a DNA sensors based on amphiphilic conjugated PPE using the signal amplification property of conjugated polymers.²⁰⁵ The 3' end of the probe DNA, amine-modified single strand 15base DNA sequence, has been covalently coupled to the carboxylic acid side of PPE in the LB film. The 5' end of target DNA labeled with hexachlorofluorescein (HEX) dye would pair with the 3' end of the probe DNA located near the PPE surface. As a result, the fluorescence emission of the PPE was quenched, while the emission of HEX ($\lambda_{\text{max}} = 557 \text{ nm}$) was amplified due to the FRET between the underlying PPE and HEX dye group on target DNA sequence.

QDs were utilized in the luminescent LB films for biosensing.⁵⁴ As shown in Fig. 13, a thin film of TOPO-ODA-ZnS-CdSe and TOPO-TDPA-ZnS-CdSe QDs was constructed by the LB technique and further modified by an amphiphilic polymer, poly(maleic anhydride-alt-1-tetradecene) (PMA), through self-assembly.

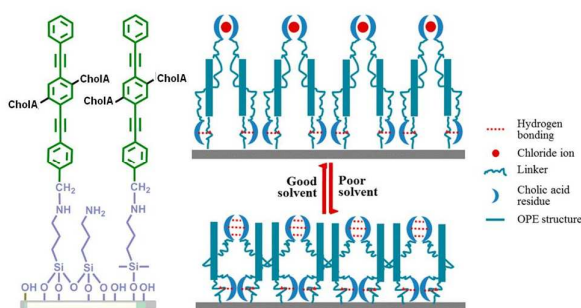


Fig. 14 Structure of SAM film of CholA-OPE and cartoon illustrating the possible change of the conformations of the surface-immobilized molecules of CholA-OPE with its medium being changed from a good solvent (acetone as an example) to a poor one (water, for example). Reproduced from ref. 213. Copyright 2012 American Chemical Society.

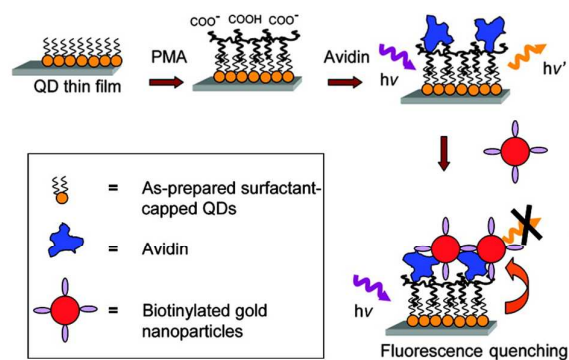


Fig. 13 Synthesis scheme of surface-modified QD thin films and the FRET between QDs and gold nanoparticles. Reproduced from ref. 54. Copyright 2008 American Chemical Society.

Then the avidin was immobilized on the PMA-coated QD film *via* electrostatic interactions. When immersed in the biotinylated gold solution, the avidin-coated QD film can attract the biotinylated gold nanoparticles by the specific interaction between avidin and biotin. The fluorescence emission of the films was quenched due to FRET between QDs and gold nanoparticles.

In conclusion, the use of LB film technique is limited by the fact that only amphiphilic compounds are capable to form monolayers at the air/water interface. Although the hydrophobic QDs are candidates to form luminescent LB films, few of them are developed for sensing application.^{206,207} Moreover, the LB system is not strongly stable exposed to the ambient environment as a result of relatively weak physical adhesion in the assembly process.²⁰⁸ Over the past several decades, the LB technique was gradually replaced by other simpler and more robust methods, such as SAM and LBL deposition.

4. Luminescent films *via* self-assembled monolayers (SAMs) method

SAM technique is based on the spontaneous molecular self-assembly *via* chemisorption on a solid surface, where molecules consist of a terminal functional group (named as “head group”) with high affinity towards the surface, a tail group arranged towards the outer surface of the film, and a spacer that connects the two units.^{209,210} The chemical or biological sensing of SAMs is determined by the tail moiety at the outer surface. In the luminescent SAMs films for chemo-/bio-sensing, the chromophores are usually immobilized on the substrate to form a monolayer as a receptor of analytes.²¹¹ Generally, the sensing of the SAM film with the one-molecule-thick layer occurs in a short response time.²¹² Nowadays, the development of SAMs in the application of luminescence sensing is the subject of interest. In this section, the current progress on the luminescent film based on the SAM technique is presented.

In recent years, some new sensors of the fluorescent SAMs were developed for chemo-sensing. For example, Fang's group fabricated a novel SAM-based fluorescent film with oligo(*p*-phenylene-ethynylene) (OPE) as a sensing unit by chemical immobilization (Fig. 14).²¹³ The introduction of cholic acid (CholA) into the side-chains of OPE prevented the aggregation of the OPE backbones and improved the solubility in organic media, promoting the covalent attachment of CholA–OPE to the silane layers on the surface of substrate. In good solvent (*e.g.*, acetone), a hydrophilic pocket formed by the hydrophilic sides of CholA could act as a holder for some small halogens anions. The protonation of the imino groups next the OPE units induced fluorescent quenching of the CholA–OPE film. Therefore, the fabricated CholA–OPE film can be used for HCl sensing in acetone-like non/less-polar solvents. However, the high sensitivity towards HCl was only observed in organic media rather than aqueous solutions, which limited its extensive application in different systems. Fortunately, the same group conducted a new fluorescent dansyl-functionalized SAM sensor suitable for different media.²¹⁴ In this system, a diamine derivative of dansyl (DNS–TOA) containing oligo-(oxyethylene) was synthesized as a linker, in which the oligo-(oxyethylene) and amine units had high affinity towards Hg^{2+} and Cu^{2+} and the dansyl group acted as the sensory element. In aqueous solution, the quenching efficiency of DNS–TOA film was slight higher towards Hg^{2+} than Cu^{2+} . However, a much higher sensitivity to Cu^{2+} was observed in acetonitrile and THF. This cross-reactive response of the film in different solvents enabled it to recognize and identify Hg^{2+} and Cu^{2+} ions, or Ni^{2+} and Co^{2+} ions.

Most of SAMs are immobilized by the treatment of the glass substrate surface with amino-functionalized trialkoxysilanes, followed by the reaction of the functional groups of target molecules. However, this kind of SAMs lacks highly ordered structures, potentially leading to the destruction of the monolayer geometry. To improve the stability of the SAM films, the efficient covalent bonding of fluorophores to silicon/glass substrates can be achieved by a proper end-functionalization. The functionalized oligothiophene structure with a triethoxysilane end can be immobilized on the hydroxylated substrates by one-step reaction (Fig. 15).²¹⁵ The β methyl groups on the inner thienyl rings can prevent π -aggregations. On the other hand, the terminal pyridine ring was sensitive to the pH values of the solutions. Therefore, the fabricated SAM film exhibited reversible red-shift emissions after exposure to acid solutions, and a fluorescent visual pH indicator can be designed for practical applications.

To improve the response performances of the film sensors, the SAM luminescent film with specific spacers was constructed.²¹⁶ The benzene rings in the spacer promoted excimer formation between terminal pyrene moieties, facilitating the direct exposure of fluorophore moieties to analytes with a fast and sensitive response. Therefore, the pyrene-functionalized SAM fluorescent film was utilized to detect PA in aqueous phase and the detection limit of the film to PA was found to be 10 nM. However, the other nitroaromatic compounds could quench the fluorescence of the films. Furthermore, in order to improve the selectivity, a SAM film with discriminatory power was designed by introducing the

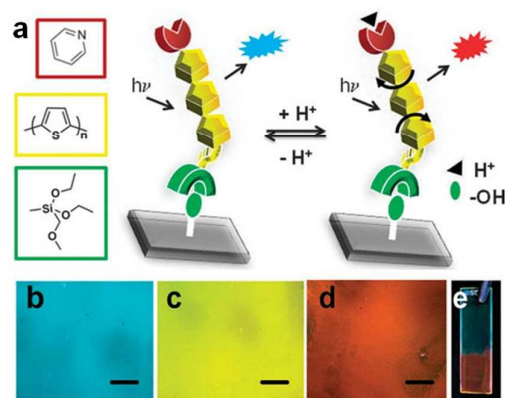


Fig. 15 (a) Molecular design strategy for the pH sensitive SAM. Red: proton antenna, yellow: fluorescent block, green: surface anchoring groups. (b, c, d) Fluorescence microscopy images (Hg lamp, $\lambda_{\text{exc}} = 330\text{--}380$ nm) of functionalized 300 nm thick SiO_2 at different pH. Bar size 250 μm . (e) Functionalized quartz (4 cm \times 1.2 cm) partially dipped in HCl/EtOH (pH = 1). Reproduced from ref. 215. Copyright 2011 The Royal Society of Chemistry.

cross-reactive sensor elements in the spacer.²¹⁷ The oligo(oxyethylene) units may provide a multidimensional microenvironment for analytes, facilitating the cross-reactive responses of this film to different nitroaromatics so that the designed SAM film provided potential in practical applications for the detection and identification of nitroaromatics with high selectivity and reversible responses.

On the other hand, the conjugated polymers as signal-transducing elements have been chemically bound on the solid surfaces to obtain a SAM film with high sensitivity.²¹⁸ The immobilization of polyfluorene was achieved by the covalent attachment of amine groups in amino-functionalized polyfluorene derivative polymer (PF– NH_2) to epoxy-terminated glass surface. The obtained SAM film showed a selective quenching response to Cu^{2+} in the concentration range of 5–50 μM . In addition, the sensing process was reversible by simply rinsing the film with an EDTA solution.

In order to extend application of conjugated polymer film in organic and aqueous media, the phosphonate-functionalized polyfluorene was synthesized to build the SAM luminescent film for sensing Fe^{3+} .²¹⁹ The hydrophobic conjugated aromatic backbones and alkyl side chains made this film available for organic media. In addition, hydrolyzation of phosphonate ester occurred in aqueous media and the formed conjugated polyelectrolyte made the surface more hydrophilic. Therefore, the luminescent film showed selective and sensitive luminescence response towards Fe^{3+} in THF and aqueous solution. The detection limits of Fe^{3+} were determined to be 2.5 μM in aqueous solution and 15 μM in THF solution, respectively.

In conclusion, the SAM films have single molecular layer, resulting in high sensitivity for chemo- and biosensing. Most covalent connections between head groups and substrates in SAM films are achieved by sulfur head compounds and silanes.²¹⁰ However, these head moieties are difficult to be synthesized. Their incompatible reactivity with other functional

groups may confine their further functionalization. Up to now, the conjugated polymers and oligomers have been successfully used in SAMs. More kinds of luminescent materials are expected for fabricating the SAM films. In addition, the introduction of other functional head groups for covalent connections may be a promising direction for luminescent SAMs.

5. Luminescent films *via* layer-by-layer (LBL) assembly

LBL assembly is one of robust and versatile technologies for preparing nano-composite thin films. Conventional LBL films are assembled by alternate adsorption of oppositely charged molecules or particles on the surface of substrate.^{220–222} Generally, negatively charged substrates (*e.g.*, glasses, quartz, silicon wafers) are initially immersed in a solution of positively charged molecules/particles, followed by washing with pure water to remove the loosely adsorbed molecules. Subsequently, the substrates are exposed to a solution of negatively charged molecules/particles and rinsed thoroughly. For positively charged substrates, analogous procedures are performed by swapping the negatively charged layer and positively charged layer. The deposition cycles are continued until the desired multilayer is achieved. The LBL technique has remarkable advantages over other assembled methods: (a) the procedures are simple and low cost without the use of any expensive, sophisticated instruments; (b) it is a suitable alternative to any type of charged components, such as polyelectrolyte, organic dye, inorganic nanomaterial and biomolecule; (c) LBL films can be fabricated with flexible choice of substrate with different matrices and shapes; (d) the film thickness with the individual layer of molecular thickness can be controlled at the nanometer scale; (e) except that a common procedure of LBL assembly is driven by electrostatic interactions, LBL assemblies are also achieved by hydrogen bonding, covalent connection, and hydrophobic interactions. These advantages allow LBL assembly technique holds the promise of fabricating uniform and robust luminescent film for practical sensing applications.

5.1 Luminescent LBL film chemosensors for heavy metal ions

Organic ligand-capped QDs are sensitive to surface interactions due to the unique discrete electronic state of each particle, and

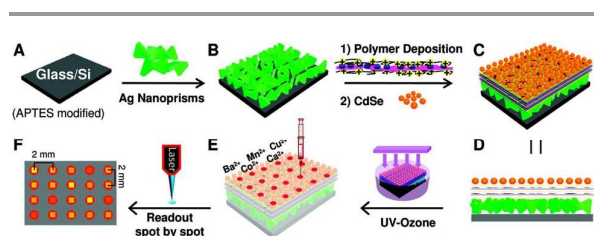


Fig. 16 Schematic diagram showing the processes of fabrication of the enhanced CdSe device for ion sensing. Reproduced from ref. 24. Copyright 2010 American Chemical Society.

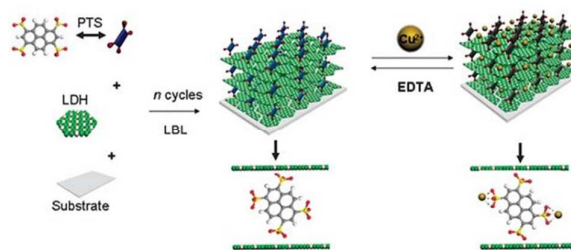


Fig. 17 The schematic representation for the measurement–regeneration cycle of the UTF. Reproduced from ref. 59. Copyright 2011 The Royal Society of Chemistry.

they have been widely used for the development of LBL luminescent sensor films.^{13,14} Mercaptosuccinic acid (MSA)-capped CdTe QDs were easy to be negative charge by altering the pH of QDs solutions. The negatively-charged CdTe QDs were then deposited on the quartz slides to form multilayer films by electrostatic interactions with PDDA.²²³ The fluorescence of PDDA/QDs multilayer films could be quenched effectively by Hg²⁺ due to the electron-transfer process between MSA molecules on the surface of QDs and Hg²⁺ ions. The quenched fluorescence intensities were perfectly described by modified Stern–Volmer equation with the concentrations of Hg²⁺ in the range of 0.01–1 μM. Note that coexisting Cu²⁺ ions showed strong interference on the detection of Hg²⁺. However, the Stern–Volmer constant for Cu²⁺ was lower than that for Hg²⁺. Therefore, the synchronous detection of Hg²⁺ and Cu²⁺ can be achieved by their different quenching constants.²²⁴ The linear ranges were obtained from 0.005 to 0.5 μM for Hg²⁺ and from 0.01 to 1 μM for Cu²⁺, respectively. In addition, the luminescence of QDs-multilayer films were able to be recovered by using GSH to remove Hg²⁺ or Cu²⁺ due to strong affinity of GSH-metal ions. Furthermore, this work was expanded to the naked-eye colorimetric readout of 5 μM of Hg²⁺ by assembling 3-mercaptopropyl acid (MPA)-coated QDs (657 nm and 553 nm) with PDDA to yield bi-color multilayer films.²²⁵ The outermost layer of the LBL luminescent film was modified by BSA through electrostatic interaction between carboxyl groups of MPA on the surface of CdTe QDs and amino groups of BSA. Interestingly, the green emission from QDs at 553 nm in the outer layer could be quenched gradually with the increase of the Hg²⁺ concentration. However, the fabricated bi-color film cannot be quenched by Cu²⁺. Therefore, the fluorescence color of this film would change from yellow-green to red. The change of color can be easily identified with the naked eyes.

More importantly, silver nanoprisms were firstly deposited on the Si or glass substrate, followed by a polymer spacer *via* LBL assembly. Finally, 16-mercaptohexadecanoic acid (16-MHA)-capped CdSe QDs were deposited as the outermost layer, and the luminescence of QDs can be enhanced by the electric field of Ag nanoprisms (Fig. 16).²⁴ The enhanced luminescence intensity of CdSe QDs was selectively quenched in the presence of Cu²⁺ as a result of the selective ion exchange processes between Cu²⁺ and Cd²⁺ on the surface of CdSe QD.

The obtained LBL luminescent film could detect Cu^{2+} within five minutes with the detection limit as low as 5 nM.

Recently, an anionic fluorescent conjugated polymer (PPESO₃) has been synthesized to fabricate fluorescence film through LBL electrostatic assembly with cationic PDDA.²²⁶ The fluorescence intensity of PDDA/PPESO₃ LBL film decreased linearly with increasing the Hg^{2+} concentration. However, other metal ions could also quench the fluorescence of PDDA/PPESO₃ LBL film owing to the weak selectivity of the electron-transfer process from the excited fluorescent dye to metal ions. Fortunately, the accurate quantification of Hg^{2+} in real water samples could be achieved when a suitable masking reagent (e.g., triethanolamine) was added to chelate the interfering ions, such as Fe^{3+} and Al^{3+} .

It is known that thermal and optical stability of the flexible polyelectrolytes are relatively poor.⁴⁷ Instead, layered inorganic materials with rigid and interlayered structure, including positively-charged layered double hydroxides (LDHs) and negatively-charged montmorillonite, could enhance the stability of the luminescent multilayer films.^{227–229} Recently, the highly ordered ultrathin film (UTF) was constructed using the positive LDH nanosheets and 1,3,6,8-pyrenetetrasulfonate acid tetrasodium (PTS) through the electrostatic LBL deposition, which was perpendicular to the substrates with a periodical layered structure (Fig. 17).⁵⁹ Some important advantages, such as a broad linear response range, good selectivity, and high stability, were obtained when the UTF was used for sensing Cu^{2+} . On the other hand, the UTF could be regenerated by the addition of EDTA to remove Cu^{2+} , providing high reusability with 20 cycles. More recently, PTS molecules were displaced by the other styrylbiphenyl derivative 2,2'-(1,2-Ethenediyl)bis[5-[[4-(diethylamino)-6-[(2,5-disulphophenyl)amino]-1,3,5-triazin-2-yl]amino] benzene sulfonic acid] hexasodium (BTBS), to fabricate a novel UTF, which was used for selectively recognizing heavy metal ions by the variable Stern–Volmer constant values.²³⁰

Some new materials have been developed for compensating the deficiencies of existing luminescent probes, such as toxicity and complicated preparation.¹⁵ For example, the negative graphitic carbon nitride (g-C₃N₄) nanosheets (blue-emissive) and the positive LDH nanoparticles were used as building blocks to fabricate multilayer film *via* LBL technique.²³¹ In the presence of Cu^{2+} and Ag^+ , the photoinduced electron-transfer from the conduction band of g-C₃N₄ to Cu^{2+} and Ag^+ could lead to the fluorescence quenching of the UTF. The fabricated film was successfully used for detecting Cu^{2+} and Ag^+ in aqueous solution and serum samples with a low detection limit of 20 nM. More interestingly, this UTF can distinguish Cu^{2+} from Ag^+ based on their different adsorption and desorption kinetics.

5.2 Luminescent LBL film chemosensors for explosives

A new type of organic-inorganic hybrid UTF was fabricated by electrostatic LBL assembly of optical brightener anionic stilbene derivatives and LDH nanosheets.²³² The luminescence of the UTFs were selectively sensitive to the nitroaromatic

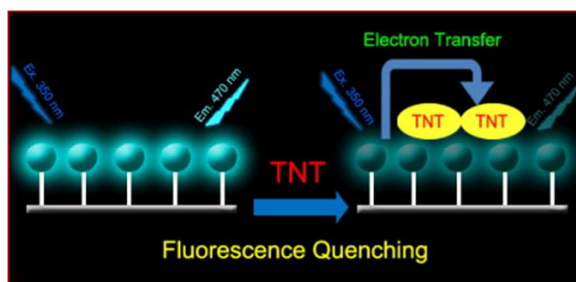


Fig. 18 Schematic representation of the photoinduced electron-transfer mechanism for the quenching of the fluorescence of one-bilayer TPE-2PhOH/PBD LBL SA film by TNT. Reproduced from ref. 233. Copyright 2011 Elsevier.

explosives. Nitroaromatic explosives could be distinguished by three fluorescent responses of the UTF: (1) the fluorescent intensity was quenched systematically upon increasing the concentration of NB and *m*-dinitrobenzene (mDNB); (2) the fluorescence intensity increased in the presence of DNT and TNT; (3) for PA, the fluorescent position showed a remarkable red-shift from 450 to 466 nm accompanied with a decrease in the fluorescence intensity. In addition, a dual-color luminescent UTF was developed by co-assembling blue BBU and orange polythiophene with LDH nanosheets.

The luminescent UTF with high stability can also be fabricated by hydrogen-bonding and covalent conjunction in the LBL process.^{220,222} For example, the one-bilayer nanofilms were self-assembled *via* hydrogen-bonding interactions between hydroxyl groups on the surface of 1,2-bis[4-(3-hydroxyphenyl)phenyl]-1,2-diphenylethane (TPE-2PhOH) and diazonium groups in 4,4'-biphenyl diazonium (BPD) salts (Fig. 18).²³³ And then, the hydrogen bonds were converted to the covalent bonds by decomposition of the diazonium groups under UV irradiations, resulting in the formation of a stable UTF. The fluorescence of TPE-2PhOH/BPD film was quenched by volatiles of four nitroanilines and the sequence of the detection sensitivities for the four nitroanilines was 3-nitroaniline (3-NA) > 4-NA > TNT > 2-NA.

In addition, the specificity of the luminescent film can be improved by the introduction of recognition elements.²¹¹ Kim *et al.* fabricated a turn-on TNT UTF through the LBL assembly using QDs as a transducing unit and engineered M13 virus as a recognition unit.²³⁴ The engineered M13 virus-trapped black hole quencher (BHQ2-COOH) could quench the emission of QDs in the UTF by energy transfer between QDs and BHQ2-COOH. Interestingly, TNT could liberate and displace BHQ2-COOH due to its higher binding affinity to the engineered M13 virus, leading to the recovery of the fluorescence in the UTF. Therefore, the prepared UTF was successfully applied to detect TNT at the sub ppb level with high sensitivity and specificity. More importantly, this nano-

composite UTF was able to differentiate TNT from DNT, which was a great challenge for explosives sensing.

5.3 Luminescent LBL film chemosensors for other analytes

Su and co-workers fabricated a gaseous formaldehyde UTF through the LBL assembly of MSA-capped CdTe QDs and polyelectrolytes (PDDA and PSS).²³⁵ As a classic electron acceptor, formaldehyde shuttled the electron from the conduction band to the valence band of the excited CdTe QDs, and thus the fluorescence of QDs in the UTF was quenched. Furthermore, BSA was used to form a protective layer on the surface of the film due to its higher binding affinity with formaldehyde than acetaldehyde. Therefore, the strong interference from acetaldehyde towards formaldehyde can be inhibited.

A luminescent porous UTF for monitoring O₂ was fabricated with assistance of mesoporous silica.²³⁶ The transition metal dyes were adsorbed into the pores of mesoporous silica particles at submonolayer coverage on the surface of the LBL film. The dyes incorporated into the mesoporous silica exhibited a stronger luminescence than them directly adsorbed on the surface of the LBL film. Interestingly, the luminescence intensities and decay lifetimes of the UTF decreased with an increase in O₂ pressure. The curved intensity Stern-Volmer plots could be fitted with two phenomenological models, a two-site model and a model based on a Freundlich binding isotherm for O₂.

The neutral luminophors can also be immobilized in the UTFs using polymers as binders.^{46,237} Recently, the LBL assembly of the neutral TPE molecules encapsulated within the poly(vinyl carbazole) (PVK) and the LDH nanosheets was achieved by hydrogen bonding interactions.²³⁷ The rigid LDH matrix could provide a stable microenvironment for the FRET process between PVK (407 nm) and TPE (465 nm). In addition, when the UTFs were exposed to the volatile organic compound (VOC) vapors, the restricted TPE molecules could become non-emissive as a result of the re-occurring of intramolecular rotations. Therefore, the layered structure UTFs exhibited reversible two-color switching of fluorescence emission by controlling the free/restricted state of TPE with different VOC vapors, such as tetrahydrofuran, acetone, toluene and chloroform.

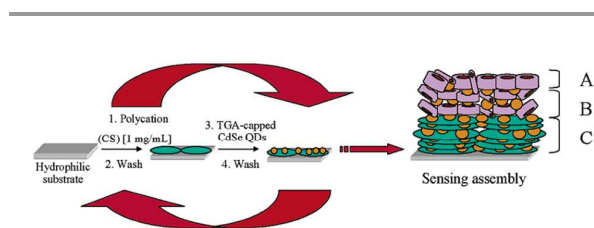


Fig. 19 Sensing assembly: (A) top layer of OPH; (B) two bilayers of OPH/TGA-capped CdSe QDs; (C) 5 bilayers of CS/TGA-capped CdSe QDs. Reproduced from ref. 238. Copyright 2003 American Chemical Society.

5.4 Luminescent LBL film biosensors

Over the past decades, the LBL luminescent films are suitable for bio-sensing owing to versatility of the LBL technique for immobilizing sensory elements with maintained activity in the solid film.²³⁸⁻²⁴² Currently, increased attention is being paid to the determination of residues of organophosphorus pesticides (OPs). For instance, a paraoxon biosensor was designed for OPs sensing by the combination of chitosan, OPH and thioglycolic acid (TGA)-capped CdSe QDs into the LBL film (Fig. 19).^{238,239} Moreover, the interaction between OPH and paraoxon led to the fluorescence quenching of the QDs in the UTF by changing the conformation of OPH. As a result, the fluorescent change could be utilized to detect paraoxon.

Tang's group developed a highly sensitive biosensor for the detection of OPs by assembling MPA-capped CdTe QDs with acetylcholinesterase enzyme (AChE) through the electrostatic LBL technique.⁴⁵ The obtained UTF can be used directly in solutions without the need of drying procedure. However, the inhibition efficiencies of the four commonly-used OPs including paraoxon, parathion, dichlorvos and omethoate to the AChE were different, resulting in inaccurate measurement in the mixture of these OPs. Therefore, the similar inhibition efficiencies towards these four OPs were highly required to improve the detection reliability. Fortunately, choline oxidase (ChOx) and AChE were introduced to fabricate bi-enzyme/QDs multilayer films for the detection of paraoxon, dichlorvos and parathion at picomolar levels (Fig. 20).²⁴⁰ Moreover, the total concentration of any two mixture among paraoxon, dichlorvos and parathion could be detected by the proposed bi-enzyme biosensor. Similarly, they developed a blood glucose sensor through alternately depositing negative MPA-capped CdTe QDs with positive GOx.⁵⁸ GOx can catalytically oxidize glucose to produce H₂O₂, leading to the luminescence quenching of QDs. The quenching rate was plotted as a function of the glucose concentration. The fabricated UTF has been successfully used for the determination of glucose in real serum samples without sample pretreatment.

In addition, the TGA-modified CdSe/ZnS QDs (540 nm) as fluorescent donors were assembled with poly(allylamine hydrochloride) (PAH) on the poly(dimethylsiloxane) surface of microfluidic channel through the LBL technique. Next, as

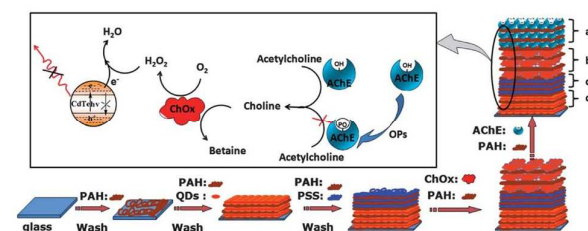


Fig. 20 Scheme of (PAH/CdTe)_x(PAH/PSS)_y(PAH/ChOx)_z(PAH/AChE)₂ biosensor: (a) top *z* bilayers of PAH/AChE, (b) *y* bilayers of PAH/ChOx, (c) intermediate 3 bilayers of PAH/PSS, and (d) bottom *x* bilayers of PAH/QDs. Reproduced from ref.240. Copyright 2011 The Royal Society of Chemistry.

fluorescent acceptors and recognition units, rhodamine (590 nm)-labeled neurotensin molecules were deposited on the outer layer of the UTF. Finally, the real-time monitoring of the enzymatic cleavage of neurotensin was successfully explored through a FRET-based luminescent film in the microfluidic channel. The ability to grow the sensing UTFs in microfluidic channels further enables us to perform the assays of cell and tissue cultures.²⁴¹ On the other hand, 8-amino-1,3,6-naphthalenetrisulfonate (ANTS) assembled into the ANTS/LDH UTF could directly recognize dextran oligosaccharides.²⁴² Moreover, the quenched luminescence can be recovered by immersing this UTF into H₂O₂ solution.

In conclusion, there is no doubt that electrostatic interaction is the most effective way to fabricate luminescent LBL films. For the neutral materials, they are needed to be encapsulated within polymer or surfactant micelles for electrostatic LBL assembly. Building blocks are preferred to any type of charged components, including polyelectrolyte, inorganic layered materials, proteins, *etc.* However, the dense 2D structure from these blocks takes negative impact on the diffusion and permeability of analytes throughout the whole film, resulting in a slow response towards target molecules, especially for vapor.²³³ Fortunately, an additional sensing layer could be deposited on the surface of luminescent LBL films. Then they can be served as an intrinsically referenced sensor films. On the other hand, it does take several hours to construct a whole UTF due to the time-consuming adsorption-desorption equilibrium (usually 10–30 min) in each assembly process.^{243–245}

6. Luminescent films *via* electrospinning

It is well-known that the performances of luminescent sensory films depend on the film thickness because the non-porous rigid structure in the luminescent films makes the diffusion of analytes slow. Therefore, the fabrication of porous films is highly desirable for improving the sensitivity.⁶⁶ The polymer solution could generate nanofibers with large surface-to-volume ratios and mechanical strength by electrospinning technique. Electrospinning is a simple deposition technique consists of four major components: a direct current power supply, a metallic spinneret, a pump-driven syringe, and a grounded collector.²⁴⁶ Extruded from a spinneret, the polymer solution initially forms a droplet. Under the influence of the high electric field, surface tension and viscosity resistance, the droplet deforms and a charged liquid ejects towards the grounded collector. The jet will be stretched by electrostatic repulsion and will whip in air medium, leading to the formation of continuous fibers on the collector. Then, a defined three-dimensional porous mesh can be formed on the plane target plate.^{247,248} The film with porous mesh is achieved by various nanofiber materials, such as polymers, ceramic precursors and organic-inorganic composites. On the other hand, the sensing elements or molecular recognition units are easy to incorporate into porous mesh for chemo-/bio-sensors.

Pei and co-workers found that the conjugated polymer exhibited a strong ACQ effect in spin-casting film.²⁴⁹ However,

the electrospinning treatment towards this synthesized polymer could quickly froze the polymer chains, effectively preventing the intermolecular π - π interactions. Next, the supporting matrix PS doping-conjugated polymer was electrospun to fabricate the electrospun optical fibrous (EOF) films for the determination of DNT vapor. Furthermore, the sensitivity can be improved by the addition of sodium dodecyl sulfate, a porogen agent, to form secondary pores into the nanofibers. This work has successfully developed a typical electrospinning technology for other conjugated polymers or materials for optical chemo-/bio-sensors. Similarly, tetrakis(4-methoxyphenyl) porphyrin (TMOPP) as sensing material was mixed with PS (supporting matrix) and Triton X-100 (porogen agent) to make an electrospun solution.²⁵⁰ Note that dodecylamine was used to strengthen attachment of the explosives onto the EOF film through the proton transfer interactions between the methyl groups of the explosives and the amino groups of dodecylamine. Accordingly, the collision probability between the explosives and TMOPP was improved, leading to a highly sensitive response to ppb levels of TNT vapor and ppt levels of PA vapor, respectively.

In addition, a similar function as “molecular wires” in the EOF film was obtained by utilizing the potential π - π stacking between pyrene and phenyl pendants of PS.²⁵¹ Note that an organic salt, tetrabutylammonium hexafluorophosphate (TBAH) was used to increase the conductivity of electrospinning solution, resulting in the formation of nanoscale fibers with good morphology. The application of the obtained EOF film was demonstrated by detecting buried explosives in soil under a handheld UV light, indicating its great potential in landmine mapping.

A more straightforward approach was to covalently attach a luminescent pH probe to a lineal copolymer (supporting matrix) to form a spinnable luminescent polymer.²⁵² Fluorescein *o*-acrylate, a pH-sensitive monomer, could be copolymerized with methyl methacrylate and hydroxyl ethyl methacrylate to produce a luminescent pH-sensitive copolymer. The DMF solution of the synthesized lineal copolymer can be directly used to fabricate the pH-sensing EOF film by electrospinning. Moreover, through the addition of charged monomers, the slightly charged copolymers were also prepared and used to form films. The excitation and emission properties of the EOF films were identical to those of the polymer solutions ($\lambda_{\text{ex/em}} = 480/535$ nm).

Typically, the luminescence of CdSe QDs can be quenched by nicotinamide adenine dinucleotide (NAD) through electron-transfer process.^{253,254} However, NAD can convert to NADH through the lactate dehydrogenase-catalyzed reaction, resulting in the recovery of the QD fluorescence. Therefore, a “turn-on” enzyme sensor for lactate dehydrogenase in the range of 200–2400 U/L was successfully fabricated (Fig. 21).²⁵⁵ On the other hand, a glucose sensor was explored by immobilizing GOx enzyme onto the (bt)₂Ir(*acac*)/PS EOF film.²⁵⁶ The luminescence intensity of (bt)₂Ir(*acac*) was effectively weakened by trace amounts of dissolved O₂. In the presence of glucose, O₂ in the interior of the GOx/EOF could efficiently react with glucose to generate H₂O₂, resulting in the enhanced

luminescence of EOF. An extremely low detection limit of glucose (0.1 nM) was achieved within 1 s.

A novel EOF film was fabricated by meso-2,6-dichlorophenyltripyrinone (TPN-Cl₂).²⁵ When the center of TPN-Cl₂ captured Zn²⁺ ions, the EOF film could emit red fluorescence. The limit of detection for Zn²⁺ was 10⁻⁶ M using this EOF film, meeting the criterion for Zn²⁺ sensing in biologic samples. Moreover, this EOF film exhibited a high sensitivity and selectivity in the commonly used cell culture liquid media (Dulbecco's modified Eagle medium and fetal bovine serum). Similarly, when SRhB was physically blended with NBD-based copolymer, the obtained mixture was electrospun to form fluorescent nanofibrous films for the ratiometric detection of Fe³⁺.²⁵⁷ In conclusion, either turn-on or ratiometric luminescent EOF films are still in their infancy, more efforts should be put on exploring their huge potential.

However, it is not always a smooth process to obtain the multicomponent EOF films by electrospinning. The direct doping could induce poor dispersion of the multiple additives and self-quenching of luminophors. As a result, the obtained EOF films exhibited worse spinnability and sensing performance.^{258,259} A straightforward solution is to functionalize the surface of the EOF films rather than the EOF films.²⁶⁰ Yang *et al.* utilized the adamantane-modified polymer to prepare EOF films through electrospinning, and then the rhodamine-cyclodextrin was adsorbed on the EOF films *via* host-guest interaction to construct a fluorescent probe for Hg²⁺ sensing (Fig. 22).²⁵⁸ The sensing process did not need the inner-layer analyte diffusion and thus the response time was so fast. Similarly, the other surface modification approaches (*e.g.*, covalent grafting and conjugation-directed adsorption) were also developed.^{259,260}

In conclusion, there are three major factors influencing the formation of EOF films: (1) polymer properties, (2) polymer solution viscosity, and (3) electrospinning parameters. Firstly, a suitable solvent is required to obtain the uniform electrospun

solution consisting of functional materials and polymer. Then, the polymer solution viscosity plays a key role to determine whether fibers can be electrospun. At last, the quantity of EOF films is affected by the above three factors. Up to now, there is no effective method to obtain the ideal parameters before electrospinning. In addition, the existence of beads is a common problem in electrospun fibres. Generally, the number of beads could be decreased by increasing the polymer concentration (Table 6).

7. Luminescent films for chemo-/bioimaging

Luminescent chemo-/bioimaging could be considered as the most straightforward application of luminescent sensing films because it is a convenient and versatile technique to visualize the distribution and quantitative analysis of analytes.²⁶¹⁻²⁶³ A typical imaging system consists of a CCD (charge coupled device) camera as the detector element, a LED array as the light source, and a set of appropriate optical filters. Different from collected data at a single point, the data of the whole sensing area were recorded with a CCD camera for yielding luminescence intensity images.²⁶⁴

There are three common readout schemes for imaging luminescent films: (1) luminescence intensity imaging, (2) luminescence lifetime imaging, and (3) ratiometric RGB imaging.²⁶⁵ At first glance, it would appear that the luminescence imaging of luminescent sensing films can be easily achieved *via* measuring luminescence intensity. However, the luminescence intensity imaging usually suffers from several inherent drawbacks, including photobleaching of the applied probes, background fluorescence of the sample, light scatter, inhomogeneous illumination, and non-uniform distribution of the probes in the sensor film.²⁶¹ Therefore, calibration and referencing based on ratiometric measurements are mandatory for ensuring the accuracy and reliability. A straightforward solution is to use the dual-wavelength probes or the analyte-insensitive luminophors as a reference.²⁶⁶ They are often called the wavelength-based ratiometric referencing techniques.

Alternatively, an intrinsically referenced method, luminescence lifetime imaging, is particularly useful. For the rapid lifetime determination method, the probes in luminescent films are excited by a short pulse of light, and the luminescence emission intensities at different delay time are captured by a CCD camera in two precisely timed gates. On the other hand, the dual lifetime determination approach requires four time gated images with different delay time.²⁶³ However, the luminescence intensity at the delay time is relatively low. Therefore, only very bright probes with long luminescent lifetimes (at least μ s) could allow their emissions recorded in the time gated mode. More discussions and examples about luminescence intensity imaging and luminescence lifetime imaging can be seen in the recent reviews by Schaeferling and Wolfbeis.^{267,102}

The ratiometric RGB imaging technique can be considered as a simple spectrometer with three different wavelength

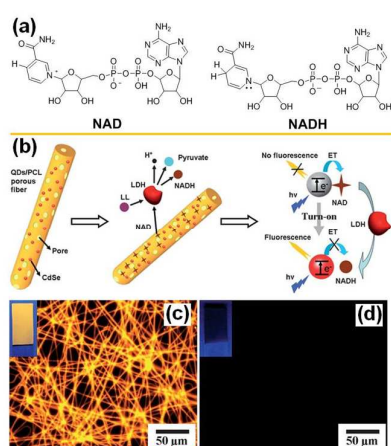


Fig. 21 The principle for assay of the activity of LDH based on CdSe QD doped fluorescent-porous fiber and enzyme-catalyzed reactions. (a) Constitutional formula of NAD and NADH; (b) Schematic of turn-on detection process; (c) fluorescence photos of films. Reproduced from ref. 227. Copyright 2012 The Royal Society of Chemistry.

(red/green/blue) filters using RGB digital cameras. In comparison with the previous wavelength-based ratiometric referencing techniques, it can fulfill the same functionality without the need of sophisticated and costly beam splitters. However, the emission peaks of the luminophors are required to match the three color channels of RGB cameras. In this basic principle, a CO₂-sensitive probe HPTS (blue emission) and a temperature-sensitive probe [Eu(dpbt)(tta)₃] (red emission) were chosen to fabricate a dual luminescent film for the simultaneous imaging of CO₂ and temperature.²⁶⁸ If an inert dye was incorporated, an enhanced precision could be obtained by dividing the luminescence intensities of the analyte-sensitive probes and the reference dye.²⁶⁹ For example, the distribution of pH and pO₂ on the skin surface could be simultaneously visualized by three kinds of dyes. The red-emissive Pt-TPFPP, the green-emissive FITC, and the blue-emissive diphenylanthracene were served as O₂, pH, and reference fluorophores, respectively.²⁷⁰ Moreover, this concept was further improved by utilizing UCPS to produce an intrinsically referenced pH sensor films without the fluorescence background interference.²⁷¹

It is worth noting that multiple sensing is usually performed using the luminescence imaging schemes, such as the wavelength-based ratiometric referencing techniques, the DLD approach, and the ratiometric RGB imaging method.^{272,273} The luminescence based multiple chemical sensing and imaging has been reviewed comprehensively by Wolfbeis.²⁷⁴

8. Conclusions

In the light of the above discussion, it is clear that luminescent films have received tremendous attention in a wider range of applications in chemo-/bio-sensing (Table 7). Various methods for assembling the luminescent films establish the foundation of these achievements. Owing to its very facile operation and general applicability, the drop-casting method is extensively employed. However, it suffers from some inborn weaknesses including poor uniformity and adhesion. The spin-coating technique could generate uniform and adhesive luminescent films, and the superior physical properties of the films by spin-coating technique are benefited for real applications; however, their sensing performances are significantly influenced by film thickness and the self-quenching degree of fluorescent probes. Fortunately, the fabrications of the porous films and molecular-scale films may reduce these disadvantages. The porous films are usually achieved using electrospinning method to generate nanofibers with large surface-to-volume ratios and a defined three-dimensional porous mesh. Note that the polymer is of crucial importance for drop-casting, spin-coating, and electrospinning because the precursor solution should own appropriate viscosity for the formation of films. On the other hand, the polymer chains could be quickly frozen in the electrospinning process, effectively inhibiting the intermolecular π - π interactions.

The molecular-scale luminescent films can be fabricated by LB, SAM and LBL techniques. Traditionally, amphiphilic

substances are capable to form LB films on hydrophobic substrates through the hydrophobic forces for a few sensing applications; however, the hydrophobic QDs might also be a candidate to fabricate luminescent LB films. In comparison with the LB technique, the SAM method is widely developed by covalent connections between luminescent probes and substrates. The SAM films possess fast response time and best sensitivity for chemo-/biosensing among all the films created *via* utilization of other methods or techniques.

The LBL assembly could generate multilayer luminescent films by conventional electrostatic interactions, hydrogen bonding, covalent connection, biological recognition or hydrophobic interactions. Various luminescence materials can be used in LBL assembled films with high stability. In comparison with the cast method, the LBL assembly is capable to control the film thickness at the molecular level precisely. Moreover, the multilayer films by LBL assembly allow much higher loadings of luminescence materials than the LB and SAM films. It is worth mentioning that the LBL assembly strategy can also be combined with other assembled techniques (*e.g.*, LB and SAM) to compensate their inherent defects. However, the extensive application of this combined strategy has not yet been fully realized. In the future, more efforts are needed to explore the huge potential in terms of the multifunction sensing devices with high sensitivity and selectivity.

Acknowledgements

This work was supported by National Basic Research Program of China (973 Program, 2014CB932103), the National Natural Foundation of China (21375006), the 973 Program (2011CBA00503), and the Fundamental Research Funds for the Central Universities (YS1406 and JD1311). We also thank Prof. Xue Duan, Beijing University of Chemical Technology, for his valuable discussion.

Notes and references

- 1 J. Jo, H. Y. Lee, W. J. Liu, A. Olasz, C.-H. Chen and D. Lee, *J. Am. Chem. Soc.*, 2012, **134**, 16000.
- 2 D. T. Quang and J. S. Kim, *Chem. Rev.*, 2010, **110**, 6280.
- 3 A. E. Hargrove, S. Nieto, T. Zhang, J. L. Sessler and E. V. Anslyn, *Chem. Rev.*, 2011, **111**, 6603.
- 4 R. M. Duke, E. B. Veale, F. M. Pfeffer, P. E. Kruger and T. Gunnlaugsson, *Chem. Soc. Rev.*, 2010, **39**, 3936.
- 5 N. Boens, V. Leen and W. Dehaen, *Chem. Soc. Rev.*, 2012, **41**, 1130.
- 6 X. Q. Chen, T. Pradhan, F. Wang, J. S. Kim and J. Yoon, *Chem. Rev.*, 2012, **112**, 1910.
- 7 D. T. McQuade, A. E. Pullen and T. M. Swager, *Chem. Rev.*, 2000, **100**, 2537.

- 8 S. W. Thomas III, G. D. Joly and T. M. Swager, *Chem. Rev.*, 2007, **107**, 1339.
- 9 A. Bajaj, O. R. Miranda, R. Phillips, I.-B. Kim, D. J. Jerry, U. H. F. Bunz and V. M. Rotello, *J. Am. Chem. Soc.*, 2010, **132**, 1018.
- 10 X. L. Feng, L. B. Liu, S. Wang and D. B. Zhu, *Chem. Soc. Rev.*, 2010, **39**, 2411.
- 11 C. L. Zhu, L. B. Liu, Q. Yang, F. T. Lv and S. Wang, *Chem. Rev.*, 2012, **112**, 4687.
- 12 X. H. Li, X. H. Gao, W. Shi and H. M. Ma, *Chem. Rev.*, 2014, **114**, 590.
- 13 R. Freeman and I. Willner, *Chem. Soc. Rev.*, 2012, **41**, 4067.
- 14 P. Wu and X.-P. Yan, *Chem. Soc. Rev.*, 2013, **42**, 5489.
- 15 J. Yao, M. Yang and Y. X. Duan, *Chem. Rev.*, 2014, **114**, 6130.
- 16 L. B. Zhang and E. K. Wang, *Nano Today*, 2014, **9**, 132.
- 17 L.-Y. Chen, C.-W. Wang, Z. Q. Yuan and H.-T. Chang, *Anal. Chem.*, 2015, **1**, 216.
- 18 G. Saikia, A. K. Dwivedi and P. K. Iyer, *Anal. Methods*, 2012, **4**, 3180.
- 19 F. F. Wang, J. Y. Wen, L. Y. Huang, J. J. Huang and J. Ouyang, *Chem. Commun.*, 2012, **48**, 7395.
- 20 C. S. He, W. P. Zhu, Y. F. Xu, T. Chen and X. H. Qian, *Anal. Chim. Acta*, 2009, **651**, 227.
- 21 L. Su, T. Shu, Z. W. Wang, J. Y. Cheng, F. Xue, C. Z. Li and X. J. Zhang, *Biosens. Bioelectron.*, 2013, **44**, 16.
- 22 L. Shi, T. Yu, L. W. Sun, H. B. Huang, X. D. Pi and X. S. Peng, *J. Mater. Chem. C*, 2014, **2**, 1971.
- 23 Z. J. Lin, F. Q. Luo, T. Q. Dong, L. Y. Zheng, Y. X. Wang, Y. W. Chi and G. N. Chen, *Analyst*, 2012, **137**, 2394.
- 24 Y.-H. Chan, J. X. Chen, Q. S. Liu, S. E. Wark, D. H. Son, and J. D. Batteas, *Anal. Chem.*, 2010, **82**, 3671.
- 25 J.-H. Syu, Y.-K. Cheng, W.-Y. Hong, H.-P. Wang, Y.-C. Lin, H.-F. Meng, H.-W. Zan, S.-F. Horng, G.-F. Chang, C.-H. Hung, Y.-C. Chiu, W.-C. Chen, M.-J. Tsai and H. Cheng, *Adv. Funct. Mater.*, 2013, **23**, 1566.
- 26 Y. Takagai, Y. Nojiri, T. Takase, W. L. Hinze, M. Butsugan and S. Igarashi, *Analyst*, 2010, **135**, 1417.
- 27 F. J. Aparicio, I. Blaszczyk-Lezak, J. R. Sánchez-Valencia, M. Alcaire, J. C. González, C. Serra, A. R. González-Elipé and A. Barranco, *J. Phys. Chem. C*, 2012, **116**, 8731.
- 28 R. Ali, T. Lang, S. M. Saleh, R. J. Meier and O. S. Wolfbeis, *Anal. Chem.*, 2011, **83**, 2846.
- 29 P. L. He and N. F. Hu, *Electroanalysis*, 2004, **16**, 1122.
- 30 H. Kong, Z. R. Ma, S. Wang, X. Y. Gong, S. C. Zhang and X. R. Zhang, *Anal. Chem.*, 2014, **86**, 7734.
- 31 U. N. Maiti, J. Lim, K. E. Lee, W. J. Lee and S. O. Kim, *Adv. Mater.*, 2014, **26**, 615.
- 32 B. L. Ma, F. Zeng, F. Y. Zheng, and S. Z. Wu, *Analyst*, 2011, **136**, 3649.
- 33 D. Lee, J. Jung, D. Bilby, M. S. Kwon, J. Yun and J. Kim, *ACS Appl. Mater. Interfaces*, 2015, **7**, 2993.
- 34 F. T. Lü, L. N. Gao, L. P. Ding, L. L. Jiang and Y. Fang, *Langmuir* 2006, **22**, 841.
- 35 B. Y. Liu, F. Zeng, Y. Liu and S. Z. Wu, *Analyst*, 2012, **137**, 1698.
- 36 B. L. Ma, S. Z. Wu and F. Zeng, *Sens. Actuators, B*, 2010, **145**, 451.
- 37 M. H. Min, X. F. Wang, Y. M. Chen, L. M. Wang, H. L. Huang and J. G. Shi, *Sens. Actuators, B*, 2013, **188**, 360.
- 38 S. M. Ji, W. H. Wu, W. T. Wu, P. Song, K. L. Han, Z. G. Wang, S. Liu, H. M. Guo and J. Z. Zhao, *J. Mater. Chem.*, 2010, **20**, 1953.
- 39 X. D. Yang, B. W. Shen, Y. N. Jiang, Z. X. Zhao, C. X. Wang, C. Ma, B. Yang and Q. Lin, *J. Mater. Chem. A*, 2013, **1**, 1201.
- 40 R. Nishiyabu, S. Ushikubo, Y. Kamiya and Y. Kubo, *J. Mater. Chem. A*, 2014, **2**, 15846.
- 41 L. Basabe-Desmonts, D. N. Reinhoudt and M. Crego-Calama, *Chem. Soc. Rev.*, 2007, **36**, 993.
- 42 W. Shi and H. M. Ma, *Chem. Commun.*, 2012, **48**, 8732.
- 43 J. Tamayo, P. M. Kosaka, J. J. Ruz, Á. San Paulo and M. Calleja, *Chem. Soc. Rev.*, 2013, **42**, 1287.
- 44 G. He, H. N. Peng, T. H. Liu, M. N. Yang, Y. Zhang and Y. Fang, *J. Mater. Chem.*, 2009, **19**, 7347.
- 45 Z. Z. Zheng, Y. L. Zhou, X. Y. Li, S. Q. Liu and Z. Y. Tang, *Biosens. Bioelectron.*, 2011, **26**, 3081.
- 46 Z. Li, J. Lu, S. D. Li, S. H. Qin and Y. M. Qin, *Adv. Mater.*, 2012, **24**, 6053.
- 47 D. P. Yan, J. Lu, M. Wei, J. B. Han, J. Ma, F. Li, D. G. Evans and X. Duan, *Angew. Chem. Int. Ed.*, 2009, **48**, 3073.
- 48 Z. J. Zhao, P. Lu, J. W. Y. Lam, Z. M. Wang, C. Y. K. Chan, H. H. Y. Sung, I. D. Williams, Y. G. Ma and B. Z. Tang, *Chem. Sci.*, 2011, **2**, 672.
- 49 W. J. Guan, J. Lu, W. J. Zhou and C. Lu, *Chem. Commun.*, 2014, **50**, 11895.
- 50 Y. Z. Liao, V. Strong, Y. Wang, X.-G. Li, X. Wang and R. B. Kaner, *Adv. Funct. Mater.*, 2012, **22**, 726.
- 51 B. Esser and T. M. Swager, *Angew. Chem. Int. Ed.*, 2010, **49**, 8872.
- 52 B. W. Xu, X. F. Wu, H. B. Li, H. Tong and L. X. Wang, *Macromolecules*, 2011, **44**, 5089.

- 53 Y. J. Zheng, J. Orbulescu, X. J. Ji, F. M. Andreopoulos, S. M. Pham and R. M. Leblanc, *J. Am. Chem. Soc.*, 2003, **125**, 2680.
- 54 A. Gole, N. R. Jana, S. T. Selvan and J. Y. Ying, *Langmuir* 2008, **24**, 8181.
- 55 Y.-R. Kim, H. J. Kim, J. S. Kim and H. Kim, *Adv. Mater.*, 2008, **20**, 4428.
- 56 B. G. Imsick, J. R. Acharya and E. E. Nesterov, *Adv. Mater.*, 2013, **25**, 120.
- 57 B. G. Imsick, J. R. Acharya and E. E. Nesterov, *Chem. Commun.*, 2013, **49**, 7043.
- 58 X. Y. Li, Y. L. Zhou, Z. Z. Zheng, X. L. Yue, Z. F. Dai, S. Q. Liu and Z. Y. Tang, *Langmuir*, 2009, **11**, 6580.
- 59 W. Y. Shi, Y. J. Lin, X. G. Kong, S. T. Zhang, Y. K. Jia, M. Wei, D. G. Evans and X. Duan, *J. Mater. Chem.*, 2011, **21**, 6088.
- 60 Y. M. Qin, J. Lu, S. D. Li, Z. Li and S. F. Zheng, *J. Phys. Chem. C*, 2014, **118**, 20538.
- 61 Y. H. Wang, B. Li, Y. H. Liu, L. M. Zhang, Q. H. Zuo, L. F. Shi and Z. M. Su, *Chem. Commun.*, 2009, 5868.
- 62 X. T. Wang, J. Q. Wang, R. Tsunashima, K. Pan, B. Cao and Y.-F. Song, *Ind. Eng. Chem. Res.*, 2013, **52**, 2598.
- 63 H. Zhou, Q. Ye, W. T. Neo, J. Song, H. Yan, Y. Zong, B. Z. Tang, T. S. A. Hor and J. W. Xu, *Chem. Commun.*, 2014, **50**, 13785.
- 64 E. G.-Nadal, J. Puigmartí-Luis and D. B. Amabilino, *Chem. Soc. Rev.*, 2008, **37**, 490.
- 65 X. Wang, W. Tian, M. Y. Liao, Y. Bando and D. Golberg, *Chem. Soc. Rev.*, 2014, **43**, 1400.
- 66 C.-L. Zhang and S.-H. Yu, *Chem. Soc. Rev.*, 2014, **43**, 4423.
- 67 P. Innocenzi and L. Malfatti, *Chem. Soc. Rev.*, 2013, **42**, 4198.
- 68 Y. Fujii, H. Atarashi, M. Hino, T. Nagamura and K. Tanaka, *ACS Appl. Mater. Interfaces*, 2009, **1**, 1856.
- 69 J. W. Jo, J. W. Jung, J. U. Lee and W. H. Jo, *ACS Nano*, 2010, **4**, 5382.
- 70 Y. Liu, X. L. Zhao, B. Cai, T. F. Pei, Y. H. Tong, Q. Xin Tang and Y. C. Liu, *Nanoscale*, 2014, **6**, 1323.
- 71 M. Cavallini, *Phys. Chem. Chem. Phys.*, 2012, **14**, 11867.
- 72 Y.-F. Huang, A. R. Inigo, C.-C. Chang, K.-C. Li, C.-F. Liang, C.-W. Chang, T.-S. Lim, S.-H. Chen, J. D. White, U.-S. Jeng, A.-C. Su, Y.-S. Huang, K.-Y. Peng, S.-A. Chen, W.-W. Pai, C.-H. Lin, A. R. Tameev, S. V. Novikov, A. V. Vannikov and W.-S. Fann, *Adv. Funct. Mater.*, 2007, **17**, 2902.
- 73 X. N. Yang, J. K. J. van Duren, R. A. J. Janssen, M. A. J. Michels and J. Loos, *Macromolecules* 2004, **37**, 2151.
- 74 T. P. Bigioni, X.-M. Lin, T. T. Nguyen, E. I. Corwin, T. A. Witten and H. M. Jaeger, *Nat. Mater.*, 2006, **5**, 265.
- 75 D. Grosso, *J. Mater. Chem.*, 2011, **21**, 17033.
- 76 K. Liu, T. H. Liu, X. L. Chen, X. H. Sun and Y. Fang, *ACS Appl. Mater. Interfaces*, 2013, **5**, 9830.
- 77 C. Glynn, D. Creedon, H. Geaney, J. O'Connell, J. D. Holmes and C. O'Dwyer, *ACS Appl. Mater. Interfaces*, 2014, **6**, 2031.
- 78 M. Faustini, A. Capobianchi, G. Varvaro and D. Grosso, *Chem. Mater.*, 2012, **24**, 1072.
- 79 C. W. Sele, B. K. C. Kjellander, B. Niesen, M. J. Thornton, J. B. P. H. van der Putten, K. Myny, H. J. Wondergem, A. Moser, R. Resel, A. J. J. M. van Breemen, N. van Aerle, P. Heremans, J. E. Anthony and G. H. Gelinck, *Adv. Mater.*, 2009, **21**, 4926.
- 80 S. Kundu, A. Kafizas, G. Hyett, A. Mills, J. A. Darr and I. P. Parkin, *J. Mater. Chem.*, 2011, **21**, 6854.
- 81 J. Hwang, N. Shoji, A. Endo and H. Daiguji, *Langmuir*, 2014, **30**, 15550.
- 82 H. Iida, M. Miki, S. Iwahana and E. Yashima, *Chem. Eur. J.*, 2014, **20**, 4257.
- 83 H. Zhou, J. S. Li, M. H. Chua, H. Yan, B. Z. Tang and J. W. Xu, *Polym. Chem.*, 2014, **5**, 5628.
- 84 J.-C. Hsu, K. Sugiyama, Y.-C. Chiu, A. Hirao and W.-C. Chen, *Macromolecules*, 2010, **43**, 7151.
- 85 T. Posati, V. Benfenati, A. Sagnella, A. Pistone, M. Nocchetti, A. Donnadio, G. Ruani, R. Zamboni and M. Muccini, *Biomacromolecules*, 2014, **15**, 158.
- 86 G. Aragay, J. Pons and A. Merkoçi, *Chem. Rev.*, 2011, **111**, 3433.
- 87 H. N. Kim, W. X. Ren, J. S. Kim and J. Yoon, *Chem. Soc. Rev.*, 2012, **41**, 3210.
- 88 N. Zhang, Y. Si, Z. Z. Sun, L. J. Chen, R. Li, Y. C. Qiao and H. Wang, *Anal. Chem.*, 2014, **86**, 11714.
- 89 P. Li, C. Y. Ji, H. W. Ma, M. Zhang and Y. F. Cheng, *Chem. Eur. J.*, 2014, **20**, 5741.
- 90 D.-M. Chen, S. Wang, H.-X. Li, X.-Z. Zhu and C.-H. Zhao, *Inorg. Chem.*, 2014, **53**, 12532.
- 91 C. Fenzl, T. Hirsch and O. S. Wolfbeis, *Angew. Chem. Int. Ed.* 2014, **53**, 3318.
- 92 A. M. Cubillas, S. Unterkofler, T. G. Euser, B. J. M. Etzold, A. C. Jones, P. J. Sadler, P. Wasserscheid and P. St.J. Russell, *Chem. Soc. Rev.*, 2013, **42**, 8629.
- 93 Y. Q. Zhang, L. J. Gao, L. P. Wen, L. P. Heng and Y. L. Song, *Phys. Chem. Chem. Phys.*, 2013, **15**, 11943.
- 94 Y. Q. Zhang, X. D. Li, L. J. Gao, J. H. Qiu, L. P. Heng, B. Z. Tang and L. Jiang, *ChemPhysChem*, 2014, **15**, 507.
- 95 N. Zhao, J. W. Y. Lam, H. H. Y. Sung, H. M. Su, I. D. Williams, K. S. Wong and B. Z. Tang, *Chem. Eur. J.*, 2014, **20**, 133.

- 96 S. Hussain, S. De and P. K. Iyer, *ACS Appl. Mater. Interfaces*, 2013, **5**, 2234.
- 97 A. Jaiswal, S. S. Ghosh and A. Chattopadhyay, *Langmuir*, 2012, **28**, 15687.
- 98 J. Liu, *TrAC, Trends Anal. Chem.*, 2014, **58**, 99.
- 99 A. George, E. S. Shibu, S. M. Maliyekkal, M. S. Bootharaju and T. Pradeep, *ACS Appl. Mater. Interfaces*, 2012, **4**, 639.
- 100 J. L. Liu, Y. Liu, Q. Liu, C. Y. Li, L. N. Sun and F. Y. Li, *J. Am. Chem. Soc.*, 2011, **133**, 15276.
- 101 H. J. Zhu, T. Yu, H. D. Xu, K. Zhang, H. Jiang, Z. P. Zhang, Z. Y. Wang and S. H. Wang, *ACS Appl. Mater. Interfaces*, 2014, **6**, 21461.
- 102 X.-D. Wang and O. S. Wolfbeis, *Chem. Soc. Rev.*, 2014, **43**, 3666.
- 103 D.-L. Ma, V. P.-Y. Ma, D. S.-H. Chan, K.-H. Leung, H.-Z. He and C.-H. Leung, *Coord. Chem. Rev.*, 2012, **256**, 3087.
- 104 V. W.-W. Yam and K. M.-C. Wong, *Chem. Commun.*, 2011, **47**, 11579.
- 105 M. Marín-Suárez, B. F. E. Curchod, I. Tavernelli, U. Rothlisberger, R. Scopelliti, I. Jung, D. Di Censo, M. Grätzel, J. F. Fernández-Sánchez, A. Fernández-Gutiérrez, M. K. Nazeeruddin and E. Baranoff, *Chem. Mater.*, 2012, **24**, 2330.
- 106 M. S. Lowry and S. Bernhard, *Chem. Eur. J.*, 2006, **12**, 7970.
- 107 Z. G. Xie, L. Q. Ma, K. E. deKrafft, A. Jin and W. B. Lin, *J. Am. Chem. Soc.*, 2010, **132**, 922.
- 108 C.-J. Lin, C.-Y. Chen, S. K. Kundu and J.-S. Yang, *Inorg. Chem.*, 2014, **53**, 737.
- 109 S. M. Ji, W. H. Wu, W. T. Wu, P. Song, K. L. Han, Z. G. Wang, S. S. Liu, H. M. Guo and J. Z. Zhao, *J. Mater. Chem.*, 2010, **20**, 1953.
- 110 C. Liu, X. L. Song, Z. G. Wang and J. S. Qiu, *ChemPlusChem*, 2014, **79**, 1472.
- 111 C. Liu, X. L. Song, X. F. Rao, Y. Xing, Z. G. Wang, J. Z. Zhao and J. S. Qiu, *Dyes Pigments*, 2014, **101**, 85.
- 112 D. E. Achatz, R. J. Meier, L. H. Fischer and O. S. Wolfbeis, *Angew. Chem. Int. Ed.*, 2011, **50**, 260.
- 113 C. A. Kelly, C. Toncelli, J. P. Kerryb and D. B. Papkovsky, *J. Mater. Chem. C*, 2014, **2**, 2169.
- 114 C. A. Kelly, C. Toncelli, M. Cruz-Romero, O. V. Arzhakov, J. P. Kerry and D. B. Papkovsky, *Mater. Design*, 2015, **77**, 110.
- 115 C.-S. Chu and C.-A. Lin, *Sens. Actuators, B*, 2014, **195**, 259.
- 116 X.-D. Wang, H.-X. Chen, T.-Y. Zhou, Z.-J. Lin, J.-B. Zeng, Z.-X. Xie, X. Chen, K.-Y. Wong, G.-N. Chen and X.-R. Wang, *Biosens. Bioelectron.*, 2009, **24**, 3702.
- 117 R. Liu, Y. K. Cai, J.-M. Park, K.-M. Ho, J. Shinar and R. Shinar, *Adv. Funct. Mater.*, 2011, **21**, 4744.
- 118 K. S. Nalwa, Y. K. Cai, A. L. Thoenig, J. Shinar, R. Shinar and S. Chaudhary, *Adv. Mater.*, 2010, **22**, 4157.
- 119 L. Wang, Y. Zhou, J. Yan, J. Wang, J. Pei and Y. Cao, *Langmuir*, 2009, **25**, 1306.
- 120 C. Vijayakumar, G. Tobin, W. Schmitt, M.-J. Kim and M. Takeuchi, *Chem. Commun.*, 2010, **46**, 874.
- 121 K. Liu, T. H. Liu, X. L. Chen, X. H. Sun and Y. Fang, *ACS Appl. Mater. Interfaces*, 2013, **5**, 9830.
- 122 C. Yu, M. Xue, K. Liu, G. Wang and Y. Fang, *Langmuir*, 2014, **30**, 1257.
- 123 M. Santiago Cintrón, O. Green and J. N. Burstyn, *Inorg. Chem.*, 2012, **51**, 2737.
- 124 C.-F. Chow, M. H. W. Lam and W.-Y. Wong, *Anal. Chem.*, 2013, **85**, 8246.
- 125 M.-S. Steiner, R. J. Meier, A. Duerkop and O. S. Wolfbeis, *Anal. Chem.*, 2010, **82**, 8402.
- 126 A. Kriltz, C. Loser, G. J. Mohr and S. Trupp, *J. Sol-Gel Sci. Technol.*, 2012, **63**, 23.
- 127 D. Wencel, M. Barczak, P. Borowski and C. McDonagh, *J. Mater. Chem.*, 2012, **22**, 11720.
- 128 C.-S. Chu and Y.-L. Lo, *Sens. Actuators, B*, 2008, **129**, 120.
- 129 P. K. Contreras-Gutierrez, S. Medina-Rodríguez, A. L. Medina-Castillo, J. F. Fernandez-Sanchez and A. Fernandez-Gutierrez, *Sens. Actuators, B*, 2013, **184**, 281.
- 130 G. J. Mohr, H. Müller, *Sens. Actuators, B*, 2015, **206**, 788.
- 131 L.-N. Sun, H. S. Peng, M. I. J. Stich, D. Achatz and O. S. Wolfbeis, *Chem. Commun.*, 2009, 5000.
- 132 R. Ali, S. M. Saleh, R. J. Meier, H. A. Azab, I. I. Abdelgawad, O. S. Wolfbeis, *Sens. Actuators, B*, 2010, **150**, 126.
- 133 H. S. Mader and O. S. Wolfbeis, *Anal. Chem.*, 2010, **82**, 5002.
- 134 M. del Barrio, S. de Marcos, V. Cebolla, J. Heiland, S. Wilhelm, T. Hirsch and J. Galbán, *Biosens. Bioelectron.*, 2014, **59**, 14.
- 135 L. X. Xie, Y. Qin and H.-Y. Chen, *Anal. Chem.*, 2012, **84**, 1969.
- 136 H. Ahn, J. Hong, S. Y. Kim, I. Choi and M. J. Park, *ACS Appl. Mater. Interfaces*, 2015, **7**, 704.
- 137 M. Xu, J.-M. Han, C. Wang, X. M. Yang, J. Pei and L. Zang, *ACS Appl. Mater. Interfaces*, 2014, **6**, 8708.
- 138 D. B. Mitzel, L. L. Kosbar, C. E. Murray, M. Copel and A. Afzali, *Nature*, 2004, **428**, 299.
- 139 N. J. Jeon, J. H. Noh, Y. C. Kim, W. S. Yang, S. Ryu and S. II Seok, *Nat. Mater.*, 2014, **13**, 897.
- 140 K. Wei Chou, H. Ullah Khan, M. R. Niazi, B. Yan, R. Li, M. M.

- Payne, J. E. Anthony, D.-M. Smilgies and A. Amassian, *J. Mater. Chem. C*, 2014, **2**, 5681.
- 141 G. A. Sotiriou, C. O. Blattmann and S. E. Pratsinis, *Adv. Funct. Mater.*, 2013, **23**, 34.
- 142 B. K. Kuila, P. Formanek and M. Stamm, *Nanoscale*, 2013, **5**, 10849.
- 143 D. Choi, B. Ahn, S. H. Kim, K. Hong, M. Ree and C. E. Park, *ACS Appl. Mater. Interfaces*, 2012, **4**, 117.
- 144 I. Chung, M.-G. Kim, J. I. Jang, J. Q. He, J. B. Ketterson and M. G. Kanatzidis, *Angew. Chem.*, 2011, **123**, 11059.
- 145 M. E. Calvo and H. Míguez, *Chemistry of Materials*, 2010, **22**, 3909.
- 146 M. P. Ramuz, M. Vosgueritchian, P. Wei, C. G. Wang, Y. L. Gao, Y. P. Wu, Y. S. Chen and Z. N. Bao, *ACS Nano*, 2012, **6**, 10384.
- 147 X. Zhang, H. J. Lu, A. M. Soutar and X. T. Zeng, *J. Mater. Chem.*, 2004, **14**, 357.
- 148 R. E. Palmer, A. P. G. Robinson and Q. Guo, *ACS Nano*, 2013, **7**, 6416.
- 149 M. E. Germain and M. J. Knapp, *Chem. Soc. Rev.*, 2009, **38**, 2543.
- 150 Y. Salinas, R. Martínez-Mañez, M. D. Marcos, F. Sancenón, A. M. Costero, M. Parra and S. Gil, *Chem. Soc. Rev.*, 2012, **41**, 1261.
- 151 S. S. Nagarkar, B. Joarder, A. K. Chaudhari, S. Mukherjee and S. K. Ghosh, *Angew. Chem. Int. Ed.*, 2013, **52**, 2881.
- 152 M. C. Rong, L. P. Lin, X. H. Song, T. T. Zhao, Y. X. Zhong, J. W. Yan, Y. R. Wang and X. Chen, *Anal. Chem.*, 2015, **87**, 1288.
- 153 H. Li, J. X. Wang, Z. L. Pan, L. Y. Cui, L. Xu, R. M. Wang, Y. L. Song and L. Jiang, *J. Mater. Chem.*, 2011, **21**, 1730.
- 154 A. Alvarez, A. Salinas-Castillo, J. M. Costa -Fernández, R. Pereiro, A. Sanz-Medel, *Trends Anal. Chem.*, 2011, **30**, 1513.
- 155 Y. Liu, R. C. Mills, J. M. Boncella and K. S. Schanze, *Langmuir*, 2001, **17**, 7452.
- 156 J.-S. Yang and T. M. Swager, *J. Am. Chem. Soc.*, 1998, **120**, 5321.
- 157 J.-S. Yang and T. M. Swager, *J. Am. Chem. Soc.*, 1998, **120**, 11864.
- 158 K. R. Ghosh, S. K. Saha, J. P. Gao and Z. Y. Wang, *Chem. Commun.*, 2014, **50**, 716.
- 159 L. C. Jia, W. P. Cai and H. Q. Wang, *J. Mater. Chem.*, 2009, **19**, 7301.
- 160 T. Naddo, Y. K. Che, W. Zhang, K. Balakrishnan, X. M. Yang, M. Yen, J. C. Zhao, J. S. Moore and L. Zang, *J. Am. Chem. Soc.*, 2007, **129**, 6978.
- 161 T. Naddo, X. M. Yang, J. Moore and L. Zang, *Sens. Actuators, B*, 2008, **134**, 287.
- 162 Y. K. Che, D. E. Gross, H. L. Huang, D. J. Yang, X. M. Yang, E. Discekici, Z. Xue, H. J. Zhao, J. S. Moore and L. Zang, *J. Am. Chem. Soc.*, 2012, **134**, 4978.
- 163 C. Y. Zhang, Y. K. Che, X. M. Yang, B. R. Bunes and L. Zang, *Chem. Commun.*, 2010, **46**, 5560.
- 164 N. Venkatramaiah, A. D. G. Firmino, F. A. Almeida Paz and J. P. C. Tomé, *Chem. Commun.*, 2014, **50**, 9683.
- 165 G. B. Demirel, B. Daglar and M. Bayindir, *Chem. Commun.*, 2013, **49**, 6140.
- 166 B. W. Xu, Y. X. Xu, X. C. Wang, H. B. Li, X. F. Wu, H. Tong and L. X. Wang, *Polym. Chem.*, 2013, **4**, 5056.
- 167 Z. C. Ding, Q. Q. Zhao, R. B. Xing, X. D. Wang, J. Q. Ding, L. X. Wang and Y. C. Han, *J. Mater. Chem. C*, 2013, **1**, 786.
- 168 A. L. Hector, *Chem. Soc. Rev.*, 2007, **36**, 1745.
- 169 M. R. N. Monton, E. M. Forsberg and J. D. Brennan, *Chem. Mater.*, 2012, **24**, 796.
- 170 A. Yildirim, H. Acar, T. S. Erkal, M. Bayindir and M. O. Guler, *ACS Appl. Mater. Interfaces*, 2011, **3**, 4159.
- 171 S. Y. Tao, G. T. Li and H. S. Zhu, *J. Mater. Chem.*, 2006, **16**, 4521.
- 172 A. Vu, J. Phillips, P. Bühlmann and A. Stein, *Chem. Mater.*, 2013, **25**, 711.
- 173 P. Beyazkilic, A. Yildirim and M. Bayindir, *ACS Appl. Mater. Interfaces*, 2014, **6**, 4997.
- 174 Q. L. Fang, J. L. Geng, B. H. Liu, D. M. Gao, F. Li, Z. Y. Wang, G. J. Guan and Z. P. Zhang, *Chem. Eur. J.*, 2009, **15**, 11507.
- 175 C. M. Deng, Q. G. He, C. He, L. Q. Shi, J. G. Cheng and T. Lin, *J. Phys. Chem. B*, 2010, **114**, 4725.
- 176 J. H. Li, C. E. Kendig and E. E. Nesterov, *J. Am. Chem. Soc.*, 2007, **129**, 15911.
- 177 T. Wagner, S. Haffer, C. Weinberger, D. Klaus and M. Tiemann, *Chem. Soc. Rev.*, 2013, **42**, 4036.
- 178 X. W. Li, X. Zhou, H. Guo, C. Wang, J. Y. Liu, P. Sun, F. M. Liu and G. Y. Lu, *ACS Appl. Mater. Interfaces*, 2014, **6**, 18661.
- 179 Y. J. Yun, W. G. Hong, N.-J. Choi, H. J. Park, S. E. Moon, B. H. Kim, K.-B. Song, Y. Jun and H.-K. Lee, *Nanoscale*, 2014, **6**, 6511.
- 180 Y. Y. Fu, L. Q. Shi, D. F. Zhu, C. He, D. Wen, Q. G. He, H. M. Cao, J. G. Cheng, *Sens. Actuators, B*, 2013, **180**, 2.
- 181 X. F. Ji, Y. Yao, J. Y. Li, X. Z. Yan and F. H. Huang, *J. Am. Chem. Soc.*, 2013, **135**, 74.
- 182 W. Lu, J. T. Zhou, K. Y. Liu, D. Chen, L. M. Jiang and Z. Q.

- Shen, *J. Mater. Chem. B*, 2013, **1**, 5014.
- 183 Z. Q. Guo, W. H. Zhu and H. Tian, *Macromolecules*, 2010, **43**, 739.
- 184 C. M. Hofmann, J. B. Essner, G. A. Baker and S. N. Baker, *Nanoscale*, 2014, **6**, 5425.
- 185 D. Aigner, S. M. Borisov, P. Petritsch and I. Klimant, *Chem. Commun.*, 2013, **49**, 2139.
- 186 L. J. Shen, X. Y. Lu, H. Tian and W. H. Zhu, *Macromolecules*, 2011, **44**, 5612.
- 187 F. L. Wang, Y. Raval, H. Y. Chen, T.-R. J. Tzeng, J. D. DesJardins and J. N. Anker, *Adv. Healthcare Mater.*, 2014, **3**, 197.
- 188 T.-S. Yoon, J. Oh, S.-H. Park, V. Kim, B. G. Jung, S.-H. Min, J. Park, T. Hyeon and K.-B. Kim, *Adv. Funct. Mater.*, 2004, **14**, 1062.
- 189 C.-Y. Kuo, Y.-Y. Chen and S.-Y. Lu, *ACS Appl. Mater. Interfaces*, 2009, **1**, 72.
- 190 M. Gsänger, E. Kirchner, M. Stolte, C. Burschka, V. Stepanenko, J. Pflaum and F. Würthner, *J. Am. Chem. Soc.*, 2014, **136**, 2351.
- 191 J. A. Zasadzinski, R. Viswanathan, L. Madsen, J. Garnæs and D. K. Schwartz, *Science*, 1994, **263**, 1726.
- 192 A. P. Girard-Egrot, S. Godoy and L. J. Blum, *Adv. Colloid Interface Sci.*, 2005, **116**, 205.
- 193 F. J. Pavinatto, L. Caseli, O. N. Oliveira and Jr., *Biomacromolecules*, 2010, **11**, 1897.
- 194 Z. H. Nie, A. Petukhova and E. Kumacheva, *Nat. Nanotech.*, 2010, **5**, 15.
- 195 C.-H. Zhou, Z.-F. Shen, L.-H. Liu and S.-M. Liu, *J. Mater. Chem.*, 2011, **21**, 15132.
- 196 B. W. K. Chu and V. W. W. Yam, *Langmuir*, 2006, **22**, 7437.
- 197 H. Sato, K. Tamura, K. Ohara, S. I. Nagaoka and A. Yamagishi, *New J. Chem.*, 2011, **35**, 394.
- 198 K. Morimoto, T. Nakae, K. Ohara, K. Tamura, S. I. Nagaoka and H. Sato, *New J. Chem.*, 2012, **36**, 2467.
- 199 H. Sato, K. Tamura, M. Taniguchi and A. Yamagishi, *New J. Chem.*, 2010, **34**, 617.
- 200 G. D. Joly, L. Geiger, S. E. Kooi and T. M. Swager, *Macromolecules*, 2006, **39**, 7175.
- 201 N. C. M. Zanona, O. N. O. Jr. and L. Caseli, *J. Colloid Interf. Sci.*, 2012, 373, 69.
- 202 D. Rodrigues, F. F. Camilo and L. Caseli, *Langmuir*, 2014, **30**, 1855.
- 203 S. V. Mello, M. Mabrouki, X. H. Cao, R. M. Leblanc, T. C. Cheng and J. J. DeFrank, *Biomacromolecules*, 2003, **4**, 968.
- 204 X. H. Cao, S. V. Mello, R. M. Leblanc, V. K. Rastogi, T. C. Cheng and J. J. DeFrank, *Colloids Surf., A*, 2004, **250**, 349.
- 205 C. C. Pun, K. Lee, H. J. Kim and J. Kim, *Macromolecules*, 2006, **39**, 7461.
- 206 C. Radhakrishnan, M. K. F. Lo, C. M. Knobler, M. A. Garcia-Garibay and H. G. Monbouquette, *Langmuir*, 2011, **27**, 2099.
- 207 K. Munechika, Y. Chen, A. F. Tillack, A. P. Kulkarni, I. Jen-La Plante, A. M. Munro and D. S. Ginger, *Nano Lett.*, 2011, **11**, 2725.
- 208 U. Lange, N. V. Roznyatovskaya and V. M. Mirsky, *Anal. Chim. Acta*, 2008, **614**, 1.
- 209 D. Bonifazi, O. Enger and F. Diederich, *Chem. Soc. Rev.*, 2007, **36**, 390.
- 210 C. Vericat, M. E. Vela, G. Benitez, P. Carro and R. C. Salvarezza, *Chem. Soc. Rev.*, 2010, **39**, 1805.
- 211 L. Ding and Y. Fang, *Chem. Soc. Rev.*, 2010, **39**, 4258.
- 212 T. H. Liu, L. P. Ding, G. He, Y. Yang, W. L. Wang and Y. Fang, *ACS Appl. Mater. Interfaces*, 2011, **3**, 1245.
- 213 H. Cui, G. He, H. Y. Wang, X. H. Sun, T. H. Liu, L. P. Ding and Y. Fang, *ACS Appl. Mater. Interfaces*, 2012, **4**, 6935.
- 214 Y. Cao, L. P. Ding, S. H. Wang, Y. Liu, J. M. Fan, W. T. Hu, P. Liu and Y. Fang, *ACS Appl. Mater. Interfaces*, 2014, **6**, 49.
- 215 M. Melucci, M. Zambianchi, L. Favaretto, V. Palermo, E. Treossi, M. Montalti, S. Bonacchi and M. Cavallini, *Chem. Commun.*, 2011, **47**, 1689.
- 216 H. Y. Du, G. He, T. H. Liu, L. P. Ding and Y. Fang, *J. Photochem. Photobiol., A*, 2011, **217**, 356.
- 217 L. P. Ding, Y. Liu, Y. Cao, L. L. Wang, Y. H. Xin and Y. Fang, *J. Mater. Chem.*, 2012, **22**, 11574.
- 218 F. T. Lv, X. L. Feng, H. W. Tang, L. B. Liu, Q. Yang and S. Wang, *Adv. Funct. Mater.*, 2011, **21**, 845.
- 219 X. F. Wu, B. W. Xu, H. Tong and L. X. Wang, *Macromolecules*, 2010, **43**, 8917.
- 220 S. Srivastava and N. A. Kotov, *Acc. Chem. Res.*, 2008, **41**, 1831.
- 221 Y. Xiang, S. F. Lu and S. P. Jiang, *Chem. Soc. Rev.*, 2012, **41**, 7291.
- 222 Y. Li, X. Wang and J. Q. Sun, *Chem. Soc. Rev.*, 2012, **41**, 5998.
- 223 C. Wang, J. W. Zhao, Y. Wang, N. Lou, Q. Ma, X. G. Su, *Sens. Actuators, B*, 2009, **139**, 476.
- 224 Q. Ma, E. Ha, F. P. Yang and X. G. Su, *Anal. Chim. Acta*, 2011, **701**, 60.
- 225 F. P. Yang, Q. Ma, W. Yu and X. G. Su, *Talanta*, 2011, **84**, 411.
- 226 Y. N. Li, H. Huang, Y. Li and X. G. Su, *Sens. Actuators, B*, 2013, **188**, 772.
- 227 R. Z. Liang, R. Tian, W. Y. Shi, Z. H. Liu, D. P. Yan, M. Wei, D.

- G. Evans and X. Duan, *Chem. Commun.*, 2013, **49**, 969.
- 228 D. P. Yan, J. Lu, J. Ma, M. Wei, D. G. Evans and X. Duan, *Angew. Chem. Int. Ed.*, 2011, **50**, 720.
- 229 W. J. Zhou, W. J. Guan and C. Lu, *Chem. Commun.*, 2014, **50**, 11370.
- 230 D. P. Yan, J. Lu, M. Wei, S. D. Li, D. G. Evans and X. Duan, *Phys. Chem. Chem. Phys.*, 2012, **14**, 8591.
- 231 H. Q. Huang, R. Chen, J. L. Ma, L. Yan, Y. Q. Zhao, Y. Wang, W. J. Zhang, J. Fan and X. F. Chen, *Chem. Commun.*, 2014, **50**, 15415.
- 232 H. Y. Ma, R. Gao, D. P. Yan, J. P. Zhao and M. Wei, *J. Mater. Chem. C*, 2013, **1**, 4128.
- 233 Y. L. Zhang, J. Xia, X. Feng, B. Tong, J. B. Shi, J. G. Zhi, Y. P. Dong and Y. Wei, *Sens. Actuators, B*, 2012, **161**, 587.
- 234 H. Jin, N. Won, B. Ahn, J. Kwag, K. Heo, J.-W. Oh, Y. T. Sun, S. G. Cho, S.-W. Lee and S. Kim, *Chem. Commun.*, 2013, **49**, 604.
- 235 Q. Ma, H. L. Cui and X. G. Su, *Biosens. Bioelectron.*, 2009, **25**, 839.
- 236 B.-H. Han, I. Manners and M. A. Winnik, *Chem. Mater.*, 2005, **17**, 3160.
- 237 Z. Li, J. Lu, Y. M. Qin, S. D. Li and S. H. Qin, *J. Mater. Chem. C*, 2013, **1**, 5944.
- 238 C. A. Constantine, K. M. Gattas-Asfura, S. V. Mello, G. Crespo, V. Rastogi, T.-C. Cheng, J. J. DeFrank and R. M. Leblanc, *Langmuir*, 2003, **19**, 9863.
- 239 C. A. Constantine, K. M. Gattas-Asfura, S. V. Mello, G. Crespo, V. Rastogi, T.-C. Cheng, J. J. DeFrank and R. M. Leblanc, *J. Phys. Chem. B*, 2003, **107**, 13762.
- 240 Z. Z. Zheng, X. Y. Li, Z. F. Dai, S. Q. Liu and Z. Y. Tang, *J. Mater. Chem.*, 2011, **21**, 16955.
- 241 G. Crivat, S. M. D. Silva, D. R. Reyes, L. E. Locascio, M. Gaitan, N. Rosenzweig and Z. Rosenzweig, *J. Am. Chem. Soc.*, 2010, **132**, 1460.
- 242 L. Jin, Z. J. Guo, T. L. Wang and M. Wei, *Sens. Actuators, B*, 2013, **177**, 145.
- 243 M. Li, J. Zhang, H.-J. Nie, M. Liao, L. Sang, W. Qiao, Z. Y. Wang, Y. G. Ma, Y.-W. Zhong and K. Ariga, *Chem. Commun.*, 2013, **49**, 6879.
- 244 J. F. Wang, Q. F. Cheng, L. Lin, L. F. Chen and L. Jiang, *Nanoscale*, 2013, **5**, 6356.
- 245 B. Peng, L. F. Tan, D. Chen, X. W. Meng and F. Q. Tang, *ACS Appl. Mater. Interfaces*, 2012, **4**, 96.
- 246 G. Zhang, M. Sun, Y. Liu, H. J. Liu, J. H. Qu and J. H. Li, *Langmuir*, 2015, **31**, 1820.
- 247 S. Agarwal, J. H. Wendorff and A. Greiner, *Adv. Mater.*, 2009, **21**, 3343.
- 248 W. Y. Liu, S. Thomopoulos and Y. N. Xia, *Adv. Healthcare Mater.*, 2012, **1**, 10.
- 249 Y. Y. Long, H. B. Chen, Y. Yang, H. M. Wang, Y. F. Yang, N. Li, K. A. Li, J. Pei and F. Liu, *Macromolecules*, 2009, **42**, 6501.
- 250 Y. F. Yang, H. M. Wang, K. Su, Y. Y. Long, Z. Peng, N. Li and F. Liu, *J. Mater. Chem.*, 2011, **21**, 11895.
- 251 Y. Wang, A. La, Y. Ding, Y. X. Liu and Y. Lei, *Adv. Funct. Mater.*, 2012, **22**, 3547.
- 252 A. L. Medina-Castillo, J. F. Fernandez-Sanchez, A. Segura-Carretero and A. Fernandez-Gutierrez, *J. Mater. Chem.*, 2011, **21**, 6742.
- 253 R. Freeman and I. Willner, *Nano Lett.*, 2009, **9**, 322.
- 254 R. Freeman, R. Gill, I. Shweky, M. Kotler, U. Banin and I. Willner, *Angew. Chem.*, 2009, **121**, 315.
- 255 X. L. He, L. F. Tan, X. L. Wu, C. M. Yan, D. Chen, X. W. Meng and F. Q. Tang, *J. Mater. Chem.*, 2012, **22**, 18471.
- 256 C. S. Zhou, Y. L. Shi, X. D. Ding, M. Li, J. J. Luo, Z. Y. Lu and D. Xiao, *Anal. Chem.*, 2013, **85**, 1171.
- 257 B.-Y. Chen, C.-C. Kuo, Y.-S. Huang, S.-T. Lu, F.-C. Liang and D.-H. Jiang, *ACS Appl. Mater. Interfaces*, 2015, **7**, 2797.
- 258 W. Wang, Y. P. Li, M. D. Sun, C. Zhou, Y. Zhang, Y. X. Li and Q. B. Yang, *Chem. Commun.*, 2012, **48**, 6040.
- 259 W. Wang, X. L. Wang, Q. B. Yang, X. L. Fei, M. D. Sun and Y. Song, *Chem. Commun.*, 2013, **49**, 4833.
- 260 S. Jo, J. Kim, J. Noh, D. Kim, G. Jang, N. Lee, E. Lee and T. S. Lee, *ACS Appl. Mater. Interfaces*, 2014, **6**, 22884.
- 261 M. I. J. Stich, S. Nagl, O. S. Wolfbeis, U. Henne and M. Schaferling, *Adv. Funct. Mater.*, 2008, **18**, 1399.
- 262 L. H. Fischer, M. I. J. Stich, O. S. Wolfbeis, N. Tian, E. Holder and M. Schaeferling, *Chem. Eur. J.*, 2009, **15**, 10857.
- 263 M. I. J. Stich, M. Schaeferling and O. S. Wolfbeis, *Adv. Mater.*, 2009, **21**, 2216.
- 264 L. H. Fischer, S. M. Borisov, M. Schaeferling, I. Klimant and O. S. Wolfbeis, *Analyst*, 2010, **135**, 1224.
- 265 R. J. Meier, L. H. Fischer, O. S. Wolfbeis and M. Schaeferling, *Sens. Actuators, B*, 2013, **177**, 500.
- 266 C. McDonagh, C. S. Burke and B. D. MacCraith, *Chem. Rev.*, 2008, **108**, 400.
- 267 M. Schaeferling, *Angew. Chem. Int. Ed.*, 2012, **51**, 3532.
- 268 M. I. J. Stich, S. M. Borisov, U. Henne and M. Schaeferling, *Sens. Actuators, B*, 2009, **139**, 204.
- 269 X.-D. Wang, R. J. Meier, M. Link and O. S. Wolfbeis, *Angew.*

- Chem. Int. Ed.*, 2010, **49**, 4907.
- 270 R. J. Meier, S. Schreml, X.-D. Wang, M. Landthaler, P. Babilas and O. S. Wolfbeis, *Angew. Chem. Int. Ed.*, 2011, **50**, 10893.
- 271 R. J. Meier, J. M. B. Simbürger, T. Soukka and M. Schäferling, *Anal. Chem.*, 2014, **86**, 5535.
- 272 S. Schreml, R. J. Meier, M. Kirschbaum, S. C. Kong, S. Gehmert, O. Felthaus, S. Küchler, J. R. Sharpe, K. Wöltje, K. T. Weiß, M. Albert, U. Seidl, J. Schröder, C. Morszeck, L. Prantl, C. Duschl, S. F. Pedersen, M. Gosau, M. Berneburg, O. S. Wolfbeis, M. Landthaler and P. Babilas, *Theranostics*, 2014, **4**, 721.
- 273 M. Larsen, S. M. Borisov, B. Grunwald, I. Klimant and R. N. Glud, *Limnol. Oceanogr.: Methods*, 2011, **9**, 348.
- 274 M. I. J. Stich, L. H. Fischer and O. S. Wolfbeis, *Chem. Soc. Rev.*, 2010, **39**, 3102.



Chem Soc Rev

REVIEW ARTICLE

Table 1 List of luminescent films for heavy metal ions sensing

Method	Probe	Matrix	$\lambda_{ex}/\lambda_{em}$	Analyte	Limit of detection	Response time	Regeneration	Stability	Ref.
Drop-/dip-casting	Rhodamine green	[P(St-AM)] PC	488/592	Hg ²⁺	4 nM	30 min	Cysteine	—	93
	HPS	[P(St-AM)] PC	350/497	Fe ³⁺	5 nM	12 min	Pure water	—	94
				Hg ²⁺	5 nM				
	TPEBe-I	—	420/640	Hg ²⁺	1 μ M	30 min	—	—	95
	PPT	PS	335/402	Hg ²⁺	1.6 μ M	—	—	—	96
	Chitosan-ZnS QDs	Chitosan	315/438	Hg ²⁺	5 ppm	15 min	—	—	97
				Ag ⁺	25 ppm				
				Pb ²⁺	5 ppm				
	BSA-Au NCs	PDDA/PSS	365/610	Cu ²⁺	—	10 min	EDTA	Immersed 24 h, stored 2 months	21
	BSA-Au NCs	—	365/650	Cu ²⁺	0.5 μ M	10 min	Histidine	Stored 6 months	23
β CD-GSH-Au NCs	Chitosan	375/690	Cu ²⁺	1 ppm	10 min	—	—	99	
Au NCs-QDs	PVA	390/520,620	Pb ²⁺	3.5 nM	11 min	—	Thermo/photostable	101	
HEMA-co-DCPDP	—	460/605	Cu ²⁺	—	5 min	P ₂ O ₇ ⁴⁻	Rinsed	183	
Spin-coating	NBD/SRhB	Sol-gel	430/528,588	Hg ²⁺	1 μ M	1 min	—	Stored 6 months	35
	BSA-AuNCs	Sol-gel	350/415,635	Hg ²⁺	0.6 nM	—	—	—	184
LB	Lipid A	—	350/524	Cu ²⁺	—	—	HCl	—	53
SAM	DNS-TOA	GPTS monolayer	350/515	Cu ²⁺	—	—	—	—	214
				Hg ²⁺					
	CP	GPTS monolayer	380/426	Cu ²⁺	5 μ M	20 min	EDTA	—	218

Review Article		Chem Soc Rev							
	CP	APTES monolayer	376/421	Fe ³⁺	2.5 μM (in H ₂ O)	6 min	NH ₃ ·H ₂ O	Immersed	219
LBL	MSA–CdTe QDs	PDDA	360/589	Hg ²⁺	0.01 μM	3 h	—	Photostable, stored 1 month	223
	MSA–CdTe QDs	PDDA	360/528	Hg ²⁺ Cu ²⁺	5 nM 0.01 μM	30 min	GSH	Stored 1 week	224
	MPA–CdTe QDs	PDDA	470/553,657	Hg ²⁺	4.5 nM	30 min	—	—	225
	MHA–CdSe QDs	PSS/PDADMAC	488/627	Cu ²⁺	5 nM	5 min	—	—	24
	CP	PDDA	400/515	Hg ²⁺	0.1 μM	30 min	cysteine	Stored 1 week	226
	PTS	LDH	340/375,394	Cu ²⁺	0.2 μM	10 s	EDTA	Photostable, stored 1 month	59
	BTBS	LDH	344/445	Hg ²⁺	—	30 s	EDTA	Photostable	230
	g–C ₃ N ₄	LDH	330/442	Cu ²⁺ Ag ⁺	20 nM 20 nM	15 min	— GSH	—	231
Electrospinning	Rhodamine derivatives	Poly(HEMA-co-NMA-co-NBD)	460/540	Fe ³⁺	10 mM	15 min	EDTA	—	257
	Rhodamine derivatives	Poly(MMA-co-ADMA)	525/584	Hg ²⁺	60 μM	< 1 min	—	Immersed 24 h	258
	Rhodamine derivatives	Poly(MMA-co-AHPA)	500/557	Cu ²⁺	1.5 μM	< 10 s	EDTA	Wide pH range	259

Table 2 List of luminescent films for O₂ sensing.

Method	Probe	Matrix	$\lambda_{ex}/\lambda_{em}$	K_{SV}	Response time	Stability	Ref.
Coating	Pt-Acetylides	PMMA	—/511,553	$33 \pm 0.5 \text{ bar}^{-1}$	—	—	108
	Ru(Phen)(bpy) ₂	IMPES-C polymer	476/669	0.35 Torr^{-1}	0.8 s	—	109
	Cyclometalated Pt(II) complex	IMPES-C polymer	470/599	0.020 Torr^{-1}	3–10 s	Thermo/photostable	110
	Cyclometalated Pt(II) complex	IMPES-C polymer	475/596	0.102 Torr^{-1}	5–10 s	Thermo/photostable	111
	UCNPs-cyclometalated Ir(III) complex	Ethyl cellulose	980/568	$0.112\%^{-1}$	10–12 s	Photostable	112
	PtTFPP/CF	Sol-gel	405/650	—	6.7 s	Photostable, Stored 7 months	115
LB	Polypyridyl Ru (II) Complex	—	485/630	$0.065\%^{-1}$	30 s	—	196
	Cationic Ir(III) complex	—	430/550	0.15 kPa^{-1}	2–5 s	—	197
	Cationic Ir(III) complexes	—	430/500,550	0.10 kPa^{-1}	—	—	198

Table 3 List of luminescent films for pH sensing.

Methods	Probes	Additives	$\lambda_{\text{ex}}/\lambda_{\text{em}}$	pH range	Response time	Stability	Ref.
Coating	pH sensitive dye	Sol-gel	430/504	4.6–9	5 min	Mechanical stability	126
	HPTS	Sol-gel	460/515	4–10	12 s	Mechanical stability	127
	UCNPs–BTB	Polyurethane hydrogel	980/545,654	6–10	< 30 s	—	131
	UCNPs–ETH 5418	PVC	980/542,656	6–11	—	—	135
	PPMI–copolymer	—	445/510,570	3–11	< 30 s	Immersing a few months	136
	Perylene bisimides	Polyurethane hydrogel	648/735	5–7	< 90 s	Photostability	185
	P(NDI–HEMA)	—	572/630	4.6–8.0	< 90 s	Immersing 1 week	186
	UCNPs–bromocresol green	Sol-gel	980/661,671	5–10	10 min	Immersing 1 month	187
SAM	Triethoxysilane-ended dye	—	360/480	1–8	—	—	215
Electrospinning	FOA-co-MMA-co-HEMA	—	480/535	6.5–10	< 4 min	—	252

Table 4 List of luminescent films for explosives sensing.

Method	Probe	Matrix	$\lambda_{ex}/\lambda_{em}$	Analyte	Quenching (%) /Exposure time	Regeneration	Stability	Ref.
Drop-/dip-casting	Benzothiophene compound	—	388/459	DNT	50/30 s	—	—	119
				TNT	50/560 s	—	—	
	Small-molecule dyes	—	390/518	DNT	91/10 min	—	—	120
				TNT	72/10 min	—	—	
	CholG-3T-Py	Chol-Ph-Chol (molecular gel)	422/525	NB	70/60 s	Air	—	121
Spin-coating	PTMSDPA	—	425/533	DNT	50/48 s	—	—	155
	CP	—	400/460	DNT	91/30 s	Methanol	Washed,	156
				TNT	50/30 s	—	heated 5 min	
	CP	—	400/460	DNT	75/10 s	—	Thermal, solvent,	157
				TNT	50/30 s	—	photostable	
	ACTC	—	340/405	DNT	90/60 s	Hydrazine	—	160
TNT				83/60 s	—	—		
ACTC	—	340/405	DMNB	73/10 s	Hydrazine	—	161	

Review Article				Chem Soc Rev				
PO	—	330/515	TNT	98/180 s	—	Photostable	164	
			TNT	86/360 s				
Py-PES	—	340/471	DNT	95/30 s	—	—	165	
			TNT	90/30 s				
			NB	58/30 s				
CP gelator	—	—/432	TNT	64/60 s	Hydrazine	—	166	
			DNT	85/60 s				
H2-BCz gel	—	300/408	TNT	77/30 min	—	—	167	
			DNT	91/30 min				
Metalloporphyrin	Mesoporous silica	420/645	TNT	56/10 s	N ₂	—	171	
TKSPP	Mesoporous silica	245/425	DNT	88/60 s	—	Stored 2 months	172	
Pyrene	Sol-gel	340/470	TNT	87.4/5 min	Water	Stored 2 months	173	
C1609 dye	Sol-gel	—/518	NB	70/10 min	—	—	174	
SOP-TiO ₂	PS	355/510	TNT	80/100 s	—	Photostable	175	
MICP	—	—/560	DNT	—	Air	Stored 3 months	176	
			TNT					
LBL	BBU	LDH	mDNB	—	Methanol	—	232	
			TNT					
			PA					
	TPE-2PhOH	BPD	350/480	NA	31/25 min	—	Stored 24 h	233
	CdSe-CdS-ZnS QDs	PDDA	—/620	TNT	—	—	—	234
Electrospinning	CP	PS	327/420	DNT	40/10 min	NH ₃ ·H ₂ O	—	249
	TMOPP	PS	424/652	DNT	38/40 min	—	Stored several months	250
	Pyrene	PS	343/470	DNT	93/6 min	—	—	251

Table 5 List of luminescent films for biosensing.

Method	Probe	Matrix	$\lambda_{ex}/\lambda_{em}$	Analyte	Limit of detection	Response time	Real sample	Stability	Ref.
Coating	PtF ₂₀ TPP/QDs	Sol-gel	390/552,647	Glucose	—	5 min	Beer and serum samples	4 °C, 2 months	116
	UCNPs/FS	Poly(acrylamide)	980/520	Glucose	< 3.3 mM	—	—	Stored several weeks	134
	Ru(II)-Ln(III) complexes	PS	365/656	Biogenic amine	10 ppb	2 h	Fish sample	—	124
	Py-1/fluorescein	Polymer Hypan	505/510,620	Biogenic amine	0.01 mM	15 min	—	Stored 3 months	125
LB	FITC-OPAA	—	—/520	DFP	1 nM	30 min	—	—	203
	FITC-OPH	—	475/520	Paraoxon	1 nM	15 min	—	—	204
	CP	—	440/557	DNA	—	—	—	—	205
LBL	TGA-CdSe QDs	Chitosan	467580	Paraoxon	1 nM	—	—	—	238,239
	MPA-CdTe QDs	PAH/PSS	380/592	Paraoxon dichlorvos	—	15 min	Apple sample	-20 °C, 1 month	240

			parathion						
	MPA-CdTe QDs	PAH/PSS	380/630	Glucose	0.5 mM	5 min	Serum	—	58
	CdSe-ZnS QDs/RhB	PAH	445/540,590	Trypsin	—	—	—	—	241
	ANTS	LDH	365/550	Dextran-40	2.7 μM	2 min	H ₂ O ₂	wide pH range	242
	MPA-CdTe QDs	PAH/PSS	380/585	Paraoxon	10.5 pM	15 min	Vegetable and Fruit samples	-20 °C, 35 days	45
				parathion	4.47 pM				
Electrospinning	TPN-Cl ₂	Poly HEMA	565/620	Zn ²⁺	1 μM	1 min	DMEM	—	25
	CdSe QDs	Polycaprolactone	400/593	Lactate dehydrogenase	200 U/L	5 min	—	4 °C, 80 days	255
	(bt) ₂ Ir(acac)	PS	330/562	Glucose	0.1 nM	< 1 s	Serum	4 °C, 6 months	256

Table 6 List of the most commonly used blending materials for each method to fabricate luminescent films.

Blending material	Method for film	Property
Polystyrene (PS)	Coating, electrospinning	Moderate permeability; good optical transparency; stable in aqueous solutions; the phenyl groups in PS enable effective co-facial π - π stacking between PS and fluorophores.
Chitosan (CS)	Coating, LBL	Biocompatible and biodegradable; excellent hydrophilicity; sufficient mechanical properties; appreciable optical transparency; polycation character. It can be used to produce stable supramolecular LBL films.
Polyelectrolytes: polycation, <i>e.g.</i> , PAH, PDDA; polyanion, <i>e.g.</i> , PSS	Coating, LBL	Biocompatible; good optical transparency; excellent hydrophilicity; highly charged. They are able to strongly absorb oppositely charged molecules and particles, and especially used for LBL assembly.
Silica sol-gel	Coating	Good compatibility; easy modification; chemical inertness; facile surface modification; tunable porosity; good optical transparency. It was the most commonly used to build porous films with excellent permeability.
Layered double hydroxides (LDHs)	LBL	Positively charged layers; long range ordered; physical rigidity; UV-light resistance; good thermostability. Positively charged LDH nanosheets can be used for LBL assembly instead of polyelectrolytes to improve the thermo and photostability of the films.
Copolymers: poly(MMA-co-ADMA), poly(MMA-co-AHPA)	Electrospinning	Negligible fluorescence emission; good thermal stability; good solubility in organic solvents; proper viscosity. They are easily processed into fibres by electrospinning.
IMPES-C polymer	Coating	Good gas compatibility; good thermostability; good mechanical and chemical stability.
Polyurethane hydrogel	Coating	Biocompatible; good optical transparency; suitable hydrophilicity.

Table 7 List of the most commonly used luminescent probes.

Probe	Properties
Traditional small organic molecules	Specially designed and synthesized; high fluorescence quantum yields; can be easily immobilized in polymer film. Prone to photobleaching; aggregation-caused quenching.
Conjugated polymers (CPs)	“Molecular wire” effect; amplified optical sensitivity; improved photostability. Complicated multi-step synthesis; small Stokes shift.
AIE organic molecules	“Aggregation-induced emission”; improved photostability; imited categories; lower fluorescence quantum yield than traditional dye.
Semiconducting quantum dots (QDs)	Size- and shape-controlled optical features; high fluorescence quantum yields; broad absorbance and narrow emission bands; large Stokes shift; high stability against photobleaching. Most of QDs are cadmium-containing (toxic); relatively large physical size.
Noble metal nanoclusters (NCs)	Biocompatible; good photostability; sub-nanometer size; scaffold-dependent tunable fluorescence. Limited categories; relatively low fluorescence quantum yield.
Luminescent transition metal complexes	Long phosphorescence lifetime; high luminescence quantum yield; large Stokes shift; modular synthesis for tuning optical properties.
Upconversion nanoparticles (UCNPs)	Excited with NIR radiation; large anti-Stokes shift; high quantum yield; photostable; tunable emission; low cytotoxicity. Limited categories